

AN ANALYTICAL MODEL OF STRENGTH LOSS IN  
FILAMENT WOUND SPHERICAL VESSELS

by

Peter Joseph Leavesley

Dissertation submitted to the Graduate Faculty of the  
Virginia Polytechnic Institute and State University in  
partial fulfillment of the requirements for the degree of

DOCTOR OF PHILOSOPHY

in

Mechanical Engineering

APPROVED:

---

C.E. Knight, Chairman

---

H.H. Mabie

---

L. Meirovitch

---

L.D. Mitchell

---

R.G. Mitchiner

October, 1983

Blacksburg, VA

## Acknowledgements

I would like to express my sincere appreciation to the members of my advisory and examination committee: Professors L.D. Mitchell, R.G. Mitchiner, H.H. Mabie, L. Meirovitch, and C.E. Knight.

I am indebted to Professor Knight, my committee chairman, for his invaluable counsel, assistance, and friendship throughout my graduate endeavors.

Support of this investigation by the Union Carbide Corporation is gratefully acknowledged.

I would also like to acknowledge the support and encouragement of Mr. and Mrs. Clarence Aull and my family during the course of this investigation.

Finally, I sincerely appreciate the support of my wife Susan, whose encouragement and tremendous patience lead to the completion of this dissertation.

## Table of Contents

	<u>Page</u>
Acknowledgements . . . . .	ii
List of Figures . . . . .	iv
List of Tables . . . . .	vi
Nomenclature . . . . .	vii
Chapter	
1      Introduction . . . . .	1
2      Mesh Generation . . . . .	12
3      Finite Element Program Development . . . . .	36
4      Analysis Procedure . . . . .	67
5      Results . . . . .	75
6      Discussion . . . . .	92
7      Conclusions - Recommendations . . . . .	104
References . . . . .	107
Appendix	
A      Input Data Files . . . . .	110
B      Partial Output Listing . . . . .	114
C      NTHICK Input Instructions . . . . .	116
D      SPHMESH Input Instructions . . . . .	119
E      COUPLE Input Instructions . . . . .	122
F      COMSPH Input Instructions . . . . .	126
G      COMSPH Program Outline . . . . .	133
VITA . . . . .	152

## List of Figures

<u>Figure</u>	<u>Page</u>
1    General Design of the Filament Wound Spherical Pressure Vessels . . . . .	3
2    Delta-Axisymmetric Pattern on a Sphere . .	13
3    Spherical Coordinates . . . . .	14
4    Band Location Coordinates . . . . .	16
5    Thickness Calculation Method (Plane View) . . . . .	18
6    Coordinate System of the Mesh Generator for the Process Model . . . . .	21
7    An Example of the Nodal Point Placement for the Fill Tube . . . . .	23
8    Start of a Layer . . . . .	26
9    An Example of Node Point Placement for the Composite Layers . . . . .	28
10   An Example of Element Numbering for the Fill Tube . . . . .	30
11   An Example of Element Numbering for the Composite Layers . . . . .	32
12   Mapping of the Quadrilateral Element into r-z Space . . . . .	42
13   Crossing of Bands within a Layer . . . . .	52
14   Three Dimensional View of the Transformation Angles BETA and SETA . . .	53
15   Material Property Transformation Matrix .	55
16   Transformation Angles BETA and SETA . . .	57
17   Strain Transformation Matrix . . . . .	59
18   Initial Stress Transformation Matrix . . .	63
19   Full Generated Mesh for the Process Model . . . . .	80

List of Figures (Continued)

<u>Figure</u>		<u>Page</u>
20	Expanded View of the Mesh around the Fill Tube . . . . .	82
21	Expanded View of the Mesh at the Change of Element Length . . . . .	83
22	Expanded View of the Mesh at the Equator . . . . .	84
23	Elements with Resultant Fiber Direction Compressive Strain . . . . .	90

## List of Tables

<u>Table</u>		<u>Page</u>
1	Average Layer Fiber Direction Stress and Strain . . . . .	88

## Nomenclature

$\{b\}$	vector of body forces
$[B]$	matrix of strain shape functions
$d_i$	$i^{\text{th}}$ degree of freedom of the element
$\{d\}$	vector of nodal displacements
$[D]$	stress-strain relationship matrix
$E$	Young's modulus of elasticity
$F_i$	$i^{\text{th}}$ force or moment applied to the element
$\{F\}$	vector of element nodal forces
$G$	modulus of rigidity
$H$	weighting coefficient
$I$	potential energy
$[J]$	Jacobian matrix
$K_{ij}$	stiffness coefficients
$[K]$	element stiffness matrix
$N$	shape function
$[N]$	matrix of shape functions
P.E.	potential energy of external loads
$r$	radial coordinate
$r, z, t$	axisymmetric coordinates
$r_i$	node point coordinate in the $r$ direction
$\{t\}$	vector of surface tractions
$[T_i]$	initial stress transformation matrix
$[T_m]$	material property transformation matrix
$[T_s]$	strain transformation matrix
$u$	displacement in the $r$ direction

$u_i$	node point displacement in the r direction
$\{u\}$	vector of displacement components in the element field
$v$	displacement in the z direction
$v_i$	node point displacement in the z direction
$vol$	volume of the element
$z_i$	node point coordinate in the z direction
$\epsilon$	strain
$\{\epsilon\}$	strain tensor
$\xi, \eta$	natural coordinates
	Poisson's ratio
$\gamma$	polar angle
$\theta$	circumferential angle
$\sigma$	stress
$\{\sigma\}$	stress tensor

#### Superscript

$e$	element
$t$	transpose
$-1$	inverse
$'$	transformed

#### Subscript

$r$	r direction
$t$	t direction
$z$	z direction
$o$	initial condition



## Chapter 1

### Introduction

#### 1.1 Introduction

High-pressure containers are used in many industries for many different applications. The containers come in different shapes and sizes depending upon the application. In most applications the weight of the container is usually of little importance, but in the aerospace industry weight is usually a prime consideration along with strength and reliability. Fabricated metal containers can easily meet the requirements of strength and reliability, but they usually carry a heavy weight penalty. A composite container consisting of a thin metal liner overwrapped by continuous filaments can also meet the requirements of strength and reliability without the weight penalty of the all-metal containers. This makes fiber reinforced composites very attractive in certain applications. However, some process variables, such as winding tension and winding pattern through their interaction with some design variables like mandrel thickness and fiber composite thickness, can greatly affect the strength of fiber composites used in the pressure vessel. It is important to understand the influence of the manufacturing process and design variables on material strength.

High-strength composites are formed by winding a continuous filament, impregnated with a resin, over a mandrel of the desired form. For example, a spherical form is shown in Fig. 1. The material strength in the direction of the fibers depends upon (among other things) the fiber strength, denier, straightness, and alignment. Fibers are wound onto the mandrel under tension to insure that they are straight. There are several process and design variables at this stage that will affect the cured composite structural strength. Three of the most important variables being winding tension, mandrel stiffness, and winding thickness. The structural strength of the composite can be impaired or degraded if some of the fibers are not straight. Fibers may buckle under the following mechanism. The winding tension in the fiber straightens it out. This tension also produces pressure on the mandrel which causes it to deflect inward. This deflection is proportional to winding tension and inversely proportional to the mandrel stiffness. This deflection will relax some of the tension in this fiber layer. relaxed. When the next layer is wound on under tension, more deflection occurs. Still more tension is lost from the first layer as well as some from the second layer. As the layers build up, more and more tension is lost from the inner layers until all tension is lost, and the inner layer undergoes compressive strain along the fiber path. Fibers in uncured resin can only withstand very small

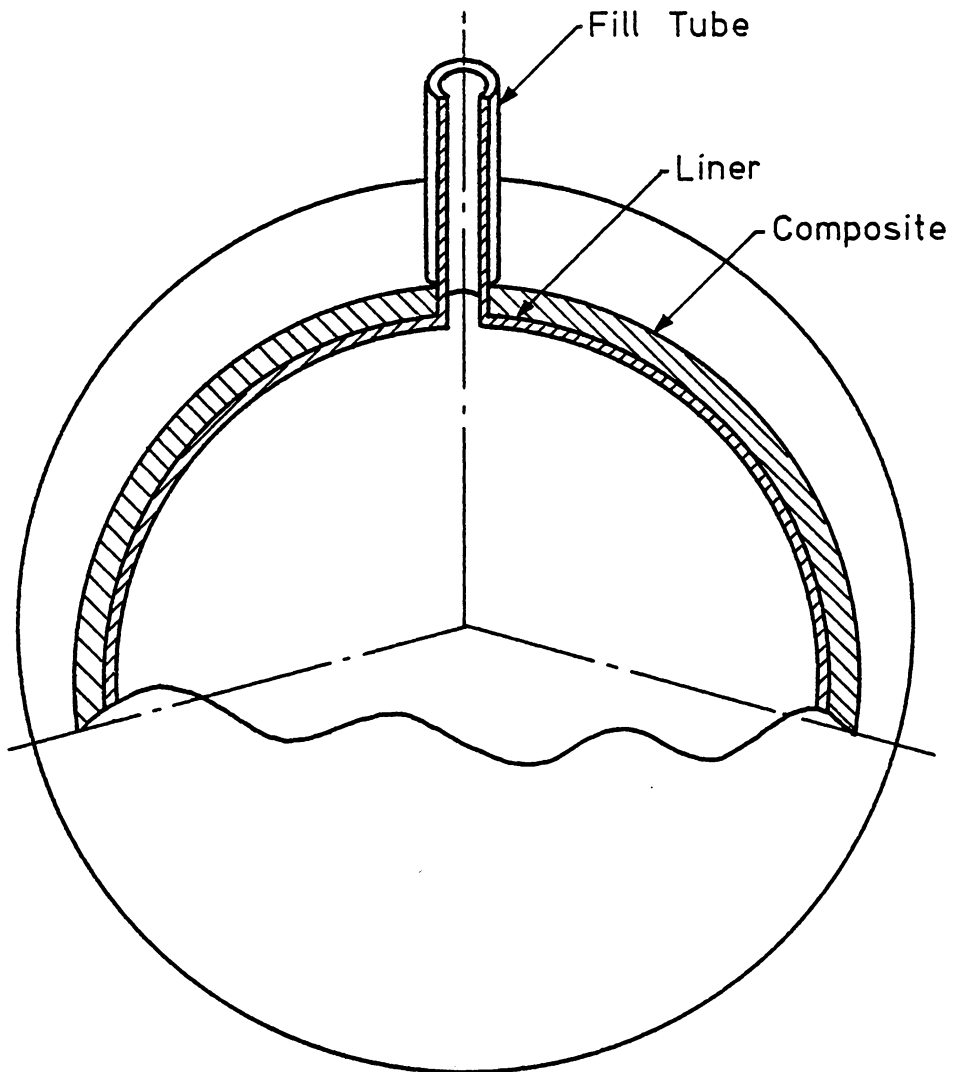


Figure 1. General Design of the Filament Wound Spherical Pressure Vessels.

amounts of axial compression without becoming wavy or without developing localized buckling. If the combination of winding tensions, mandrel stiffness, and winding thickness cause some of the inner layers in the composite to have localized buckling, the strength of the composite will be degraded. A method for analyzing this condition is needed.

## 1.2 Research Approach

The main objective of this study is to create a process model to find the fabricated strain state of the wound layers making up the sphere.

In order to create a process model, some simplification of the actual sphere is necessary. One simplification is to assume that the sphere is axisymmetric about a line passing through the center of the fill tube. Another simplification assumes that the sphere is symmetric about the equatorial plane.

The composite sphere is made by winding band sets of fibers onto a spherical form. It takes several bands in each set to create a pseudo-axisymmetric layer of fibers which usually provides full coverage at the equator of the sphere. Multiple layers are wound in the delta-axisymmetric pattern to form a design fiber thickness over the whole

sphere. The delta-axisymmetric pattern is described numerically in Appendix A and is illustrated in Fig. 2.

In order to model this fabrication process, the mathematical model must be able to analyze incrementally as the fabrication proceeds. One way of creating an incremental model is to use a finite element model of the finished structure and allow the elements to be switched on or off as required. All the elements are used to form the overall stiffness matrix. Switching off of elements is accomplished by reducing its stiffness by the order of  $(10)^6$ . This reduced stiffness when added to the assembled stiffness matrix of turned on elements has little effect. Thus the model effectively includes only the elements necessary to model the sphere at that point in its fabrication. The switching on or off of the elements probably should be performed layer-by-layer as opposed to element-by-element or band-by-band in accordance with the axisymmetric assumptions. At the beginning of fabrication only the form elements would be switched on, while the composite elements are off.

The finite element program assembles its equations in a global coordinate system, but each element of the fiber composite must have a local coordinate system aligned with the fiber direction. To assemble the structural stiffness matrix from all the elemental stiffnesses, transformation of

material properties is necessary. The transformation of initial stresses from local to global coordinates is also necessary in order to obtain the nodal loading each layer applies. The output from the finite element program should be in fiber directions, so the resultant elemental stresses and strains must be transformed back from global to local coordinates.

The final stage of the study would be to examine the strain results to find layers which have lost all their initial winding tension (identified by negative strains). Combined with the results from reference 1 a structural strength map of the sphere can be created. The results from this previous study allow one to assign a strength to a layer based upon the average strain loss within that layer. The strength is then known for every layer of the sphere after it has been manufactured. Using the Weibull statistical failure theory from reference 2, the performance or ultimate strength of the sphere can be predicted. Perhaps even some design modifications may become apparent to improve the sphere's performance.

A mesh generating program would greatly reduce the amount of work to be done in preparing data for the finite element program. The mesh generating program should use the layer profiles in forming the elements, since the fibers would be in different directions in neighboring layers. Using the

layer boundaries to form element edges would help in the switching on and off of elements layer-by-layer.

### 1.3 Review of Literature

The literature search is divided into four topical areas: 1)finite element programs and specialized elements, 2)the analysis of metallic - fiber composites, 3)incremental finite element procedures, and 4)automatic mesh generation.

The calculation of residual strains in the layers of a composite sphere, due to the fabrication process, requires a specialized finite element program. The finite element program STAP as presented by Bathe and Wilson (3)\* was chosen as the foundation for the development of the program. A one-dimensional truss element was the only element implemented in STAP. Many element formulations suitable for the analysis of axisymmetric bodies are available. Many authors (4,5,6,7,8) present a wide variety of shell elements based on an almost as wide variety of theories. All the elements of the above references have a large number of degrees of freedom. This when coupled with the large number of elements needed, would require very large amounts of storage and long execution times on the computer. The

\* Numbers in parentheses indicate reference listed at the end of this Dissertation.

element chosen to be used in the analysis of the spheres is an axisymmetric, four-noded, two-dimensional, isoparametric element capable of handling both isotropic and orthotropic materials. The four-noded quadrilateral element is an efficient, simple element which allows great flexibility in material property variation from element to element without constraining the form of the variation. The element development follows the concepts presented by Cook (9) and Zienkiewicz (10).

The finite element analysis of filament reinforced metallic-spherical pressure vessels has been carried out by Chen and Clewlow (11) and by Knight (12,13). Both modeled the final fabricated sphere by covering the form-composite with a fine mesh of elements with no regard to internal winding layer boundaries. Average material properties were then assigned to individual elements or groups of elements with no account being made for any fabrication stresses.

The analysis of fabrication stresses in structures using an incremental finite element procedure has been carried out by Clough and Woodward (14) and by Duncan and Clough (15). Their work on the analysis of large earth embankments and locks, has shown that, if the soil is assumed to be linear elastic, the calculation of stresses and displacements are closer to the measured values if an incremental loading procedure is used as opposed to a one-step method. The



incremental procedure adds or removes both element stiffness and nodal loads in each step, which simulates the actual addition or removal of soil of the structure as it is being constructed. The one-step method models the final shape of the structure and applies all the nodal loads in a single step. This method is obviously incorrect in modeling a structure with changing material volume.

In a filament wound composite the effects of varying winding tension on composite strength was examined by Portnov and Spridzans (16). They showed that the cured modulus of elasticity and the burst pressure of rings increased with increased winding tension until the formulation of cracks due to increasing radial stresses. The interaction between winding tension, mandrel stiffness, and winding thickness for filament-wound cylinders has been studied by Dobie, Leavesley and Knight (1). They found a hyperbolic relationship between the residual layer tension and the winding or spool tension. There was a spool tension below which no residual tension existed. Using this correlation and an incremental finite element program the final stress/strain state in each layer was found. Some of the inner layers were found to be in compressive hoop strain. This caused localized buckling of the fibers reducing the composite's strength.

Cain and Knight (17) examined the general form of the

Weibull statistical failure theory and present an integral form which may be used in a finite element code to determine the predicted failure of a composite structure. The tensile strength of composites can be measured by the Split-D test. Further work by Knight (18) shows that the Weibull Statistical failure theory in conjunction with finite element stress analysis of the Split-D test, provided a reasonable estimate and explanation for the lack of influence of the high stress concentrations on the results.

The structure to be analyzed by the finite element method must be simulated with a mesh of elements. This mesh is usually created by hand on small simple structures, using only a few elements, but as the number of elements grows this task becomes increasingly tedious. Most finite element programs developed to tackle large problems usually incorporate or have associated with them automatic mesh generators. There are numerous automatic mesh generation schemes available which cover the structure from boundary to boundary with a uniform mesh as presented by several authors (19,20,21,22). In this study it is desired to restrict elements from crossing internal winding layer boundaries. This made none of the above schemes suitable. The mesh generator developed by Kalkani (23) presents an approach to overcome this restriction. His mesh generator was used in the finite element analysis of earth dams. The scheme developed by Kalkani (23) uses line, triangular and

quadrilateral elements to generate the mesh. The surface line and the interlayer structural boundary lines are input by specifying characteristic points on each line. The geologic structure is divided into sections by generating vertical and horizontal lines. Elements are formed by generating vertical and horizontal lines at intervals of the element width specified for each section and by using the geologic boundary lines as element sides when they are approached. One limitation of his mesh generator was that internal boundaries could only vary linearly. However, his approach provides some guidelines for developing a mesh generator for wound spheres.

## Chapter 2

### Mesh Generation

#### 2.1 Pattern Definition

The delta-axisymmetric pattern can be designed to yield a uniform distribution of fiber orientations and uniform total thickness over most of the surface of the sphere. The delta-axisymmetric pattern is illustrated in Fig. 2. The lines in the sketch represent the edges of the band sets which are equally spaced around the polar axis. The spherical coordinate system is shown in Fig. 3. Coordinates are defined using a polar axis and a reference plane through that axis. Longitudinal lines run from pole to pole on the surface of the sphere and lie in a plane passing through the polar axis. Latitudes are circles on the sphere surface with centers lying on the polar axis.

A point on the surface of the sphere can be located by specifying the polar angle,  $\gamma$ , and the circumferential angle,  $\theta$ . The polar angle is the angle between the polar axis and the radius to the point on the longitude, and the circumferential angle is the angle between the reference plane and the longitudinal plane through the point reached.

Total coverage of the spherical surface with the design thickness is used to define the basic pattern. The number

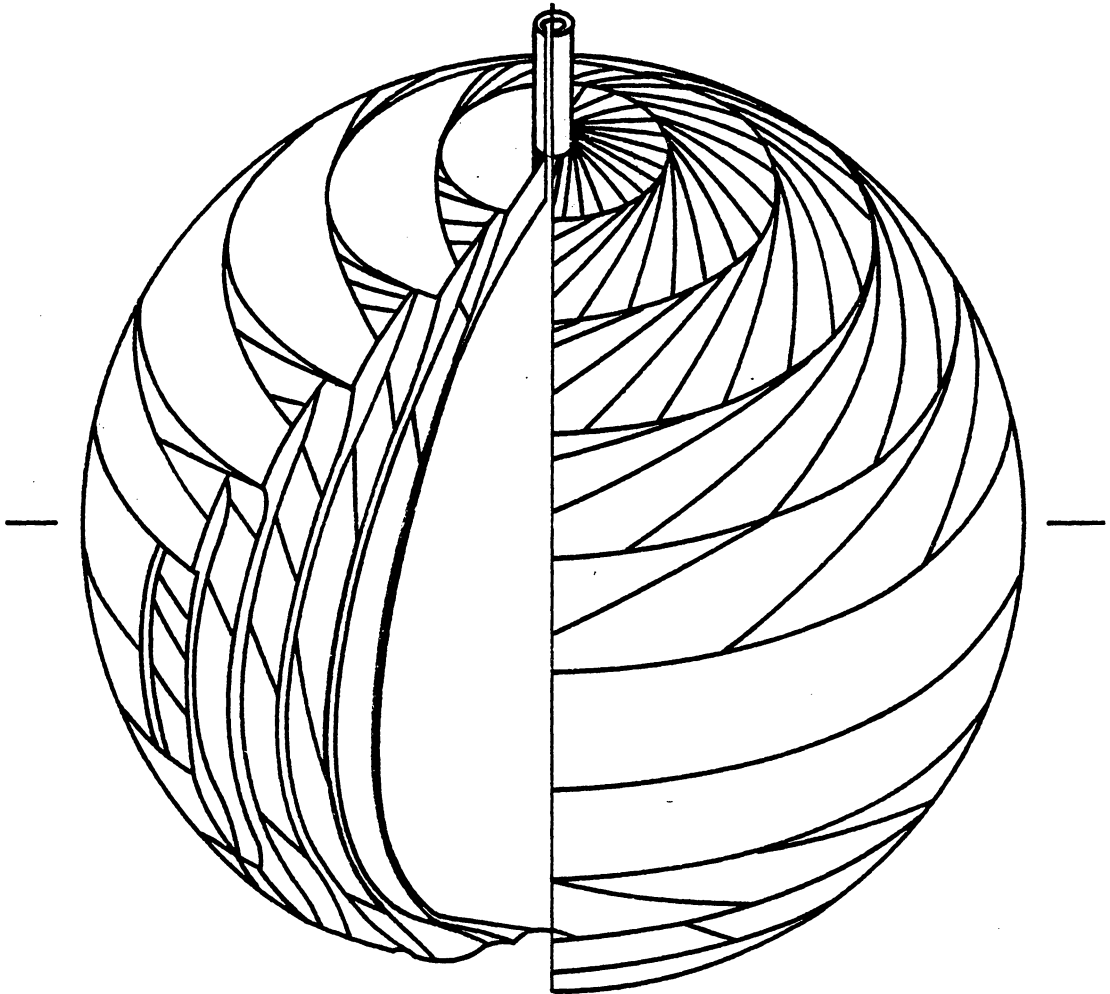


Figure 2. Delta-Axisymmetric Pattern on a Sphere.

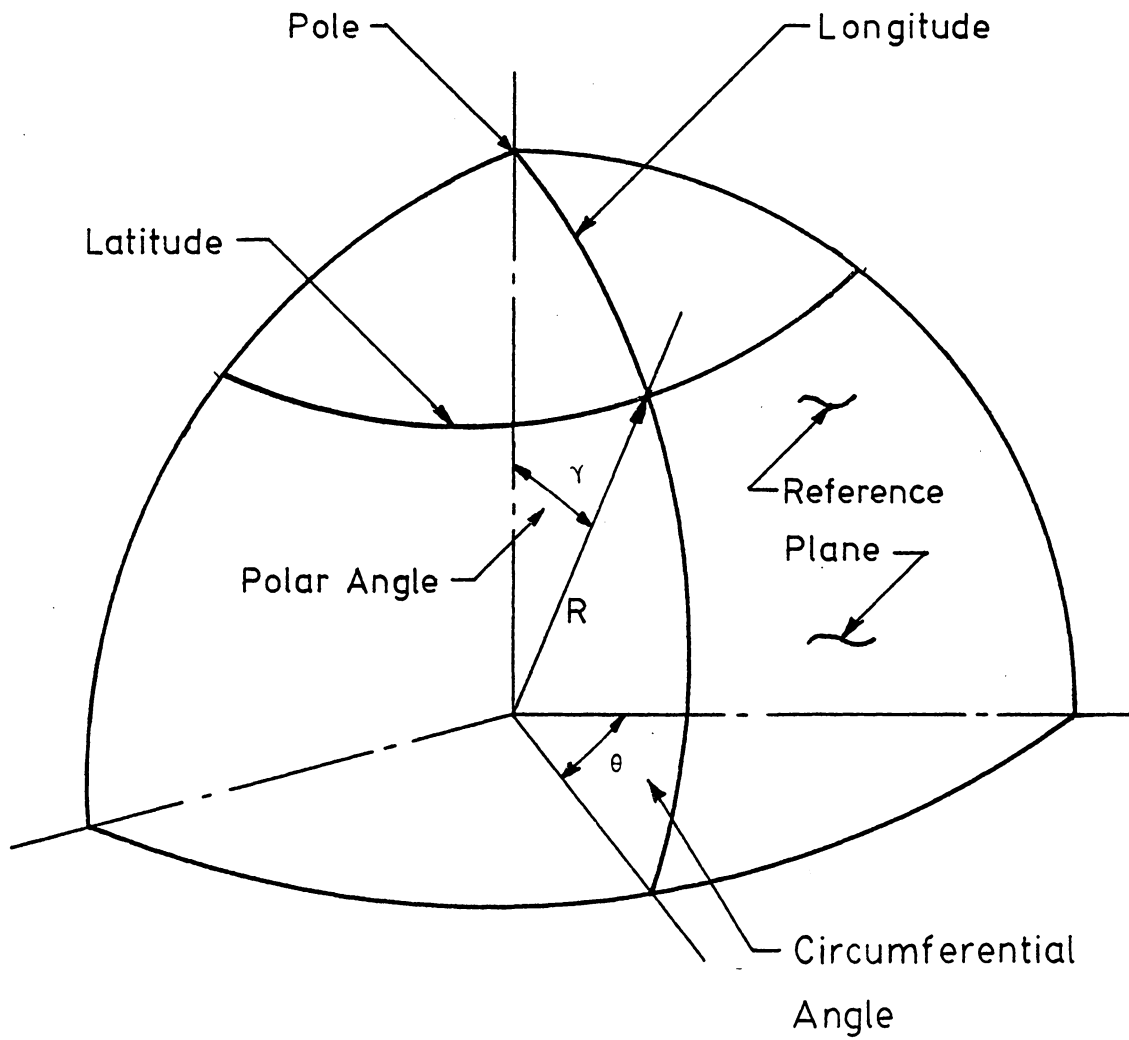


Figure 3. Spherical Coordinates.

of band sets is found by dividing the design thickness by two times the thickness of a single band. Each band set gives two layers of coverage. The sets are applied equally spaced from pole to equator along a longitudinal line. The band width is equal to the spacing along this longitudinal line. The number of bands in each set to give side by side coverage at the equator is related to their position along the longitudinal line. The first set of bands in the basic pattern are placed with one edge tangent to the polar axis, and the other edge then lies on the longitudinal line one bandwidth away. Adjustments are required to incorporate a fill tube. The center of the band lies just off a great circle of the sphere as shown in Fig. 4 and is defined by the polar angle to the inner edge,  $\gamma_1$ , and by the polar angle to the outer edge in the other hemisphere,  $\gamma_3$ . A band is formed by circumferential winding parallel to and on both sides of a great circle path. The band is started at the specified location of the band edge on one side of the great circle and circumferentially wound in a helical path at the correct band lead rate for the fiber being used until the correct band width is reached. The angle between the band center and the equator is  $\frac{\pi}{2} - \gamma_2$  and the length of the equator covered by one band is the bandwidth divided by  $\sin(\frac{\pi}{2} - \gamma_2)$ . The number of bands in this set is 360 divided by this coverage. The second set of bands is applied with one edge tangent to the longitude circle of the first set

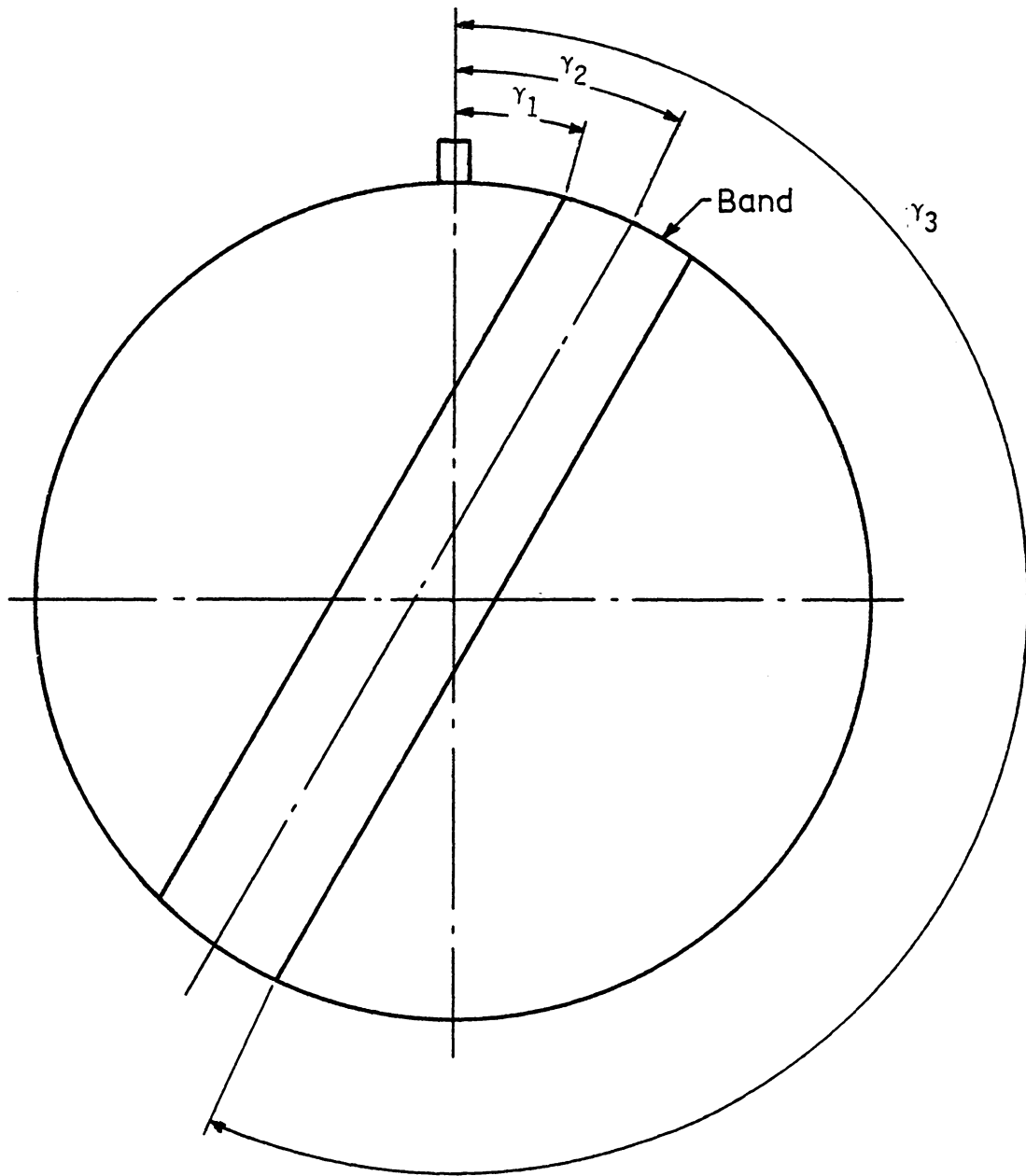


Figure 4. Band Location Coordinates.



and its other edge being one bandwidth further away. This set of bands would require slightly fewer bands than the first set to provide full coverage of the equator. Similarly, the other sets are applied progressively along the longitudinal line to the equator.

## 2.2 Pattern Simulation

The mesh generating program requires as inputs the layer thicknesses and the fiber orientation angles at all polar angles where nodes and elements are to be generated. A pattern-simulation computer program, NTHICK, written by Dr. C.E. Knight (12) was modified to provide this information. In order to generate this data, the program must calculate the thickness buildup for each band set and the fiber orientation angle with respect to the overall spherical coordinates at all specified points in the composite.

The calculations are performed by spherical geometry methods. A view of the geometry along the polar axis (axis of symmetry) is shown in Fig. 5. The concentric circles are latitudes of the sphere and the straight lines represent the coverage of a single band. The arc length along the latitude covered by a band is calculated. This is called the "BAND ARC COVERAGE". The thickness build up for a band set at a given latitude is given by the band arc coverage times the band thickness times the number of bands in the set divided by the circumference of the latitude. The fiber

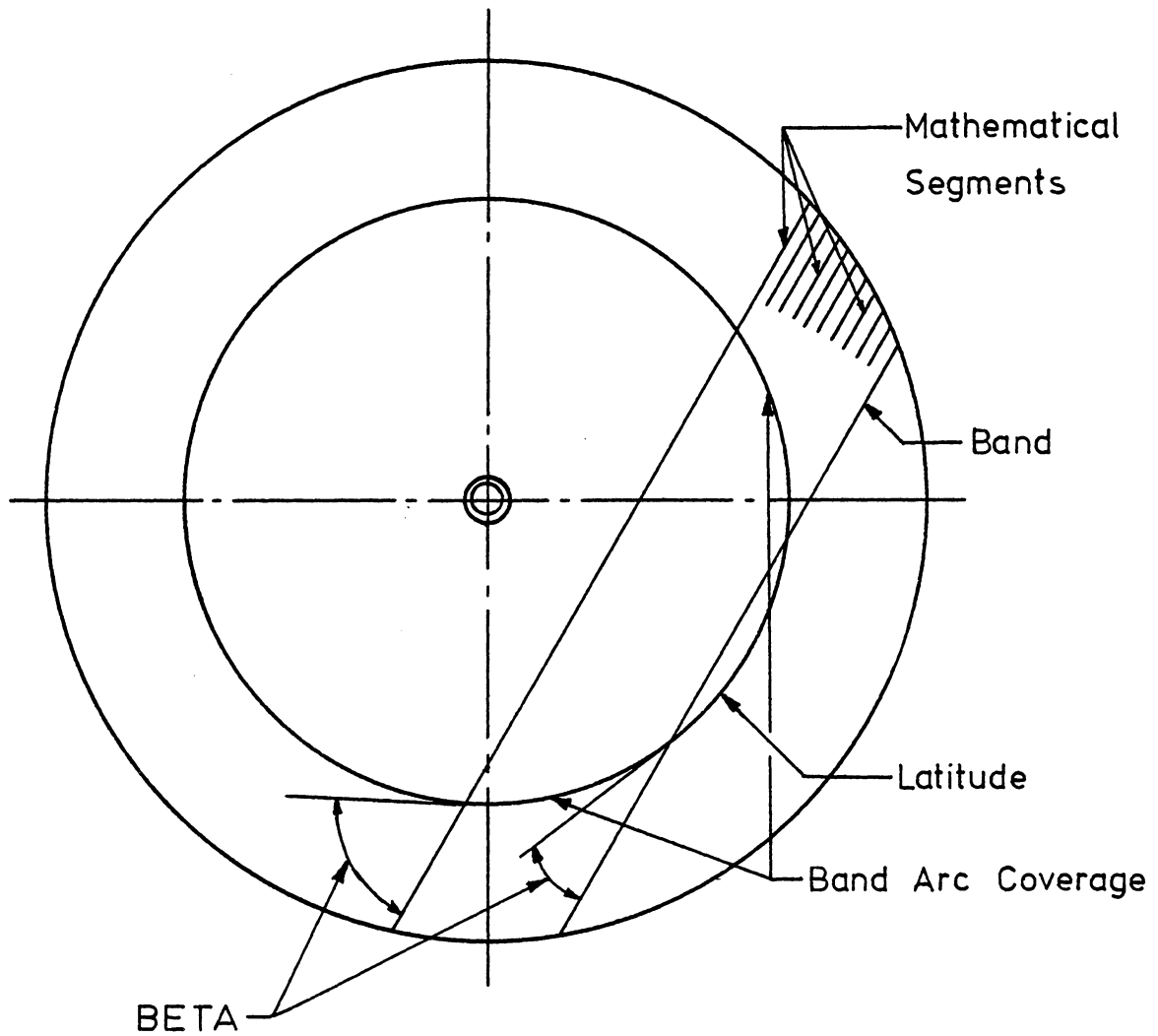


Figure 5. Thickness Calculation Method. (Plane View)

orientation angle, BETA, is the angle between the fiber direction and the latitude line. It can be determined at any point across the band, and it will vary across the band. The program calculates the fiber angle at the inner and outer edges of the band. This will be used by the mesh generating program to assign fiber orientation angles to each element. The thickness buildup is calculated for each band set and is summed to obtain the total thickness profile. The output from the program is a set of data which specifies at determined polar angular positions, PANG; 1) the thickness of every band set, 2) their associated inner and outer fiber orientation angles, BETA, as shown in Fig. 5, and 3) the total thickness profile.

### 2.3 Mesh Generator

Approximations of the contours of the bands of fibers that make up the spherical model, together with the accuracy required, force a fine mesh or a large number of elements to be used. Specifying the locations of all the node points and the formulation of the elements is tedious with a high probability of human error. Reductions of this effort and reductions in the probability of human error can be made with the use of mesh generating programs.

A mesh generating program called SPHMESH was developed specifically for the analysis of a filament wound sphere. The main constraint for element generation being that no

elements can cross band set layer boundaries. The layer boundaries are defined mathematically in the thickness program and are input into the mesh generating program. The program performs two main tasks, node point generation and element generation. The mesh generation program performs three other tasks; 1)it assigns to every element a polar angle, PANG, 2)fiber orientation angles, BETA, are assigned to all elements of the filament composite, and 3)it computes fiber lengths for all the elements within the composite. The fiber lengths are used in the finite element program COMSPH, to calculate the average fiber path strain along a band path.

The program also has the capability of drawing the generated mesh on the screen of a graphics terminal and making a hard copy of it. The mesh is drawn in the r-z coordinate system as illustrated schematically in Fig. 6 where boundaries of layers and form are sketched. There are two choices of output from the program. One gives all the output in a file printable for user inspection, and the second gives the output using an unformatted write or binary file to be read by the program COUPLE to form the input for the finite element analysis program, COMSPH.

#### 2.3.1 Node Point Generation

This part of the program generates the locations of the node points for the finite element model. The program

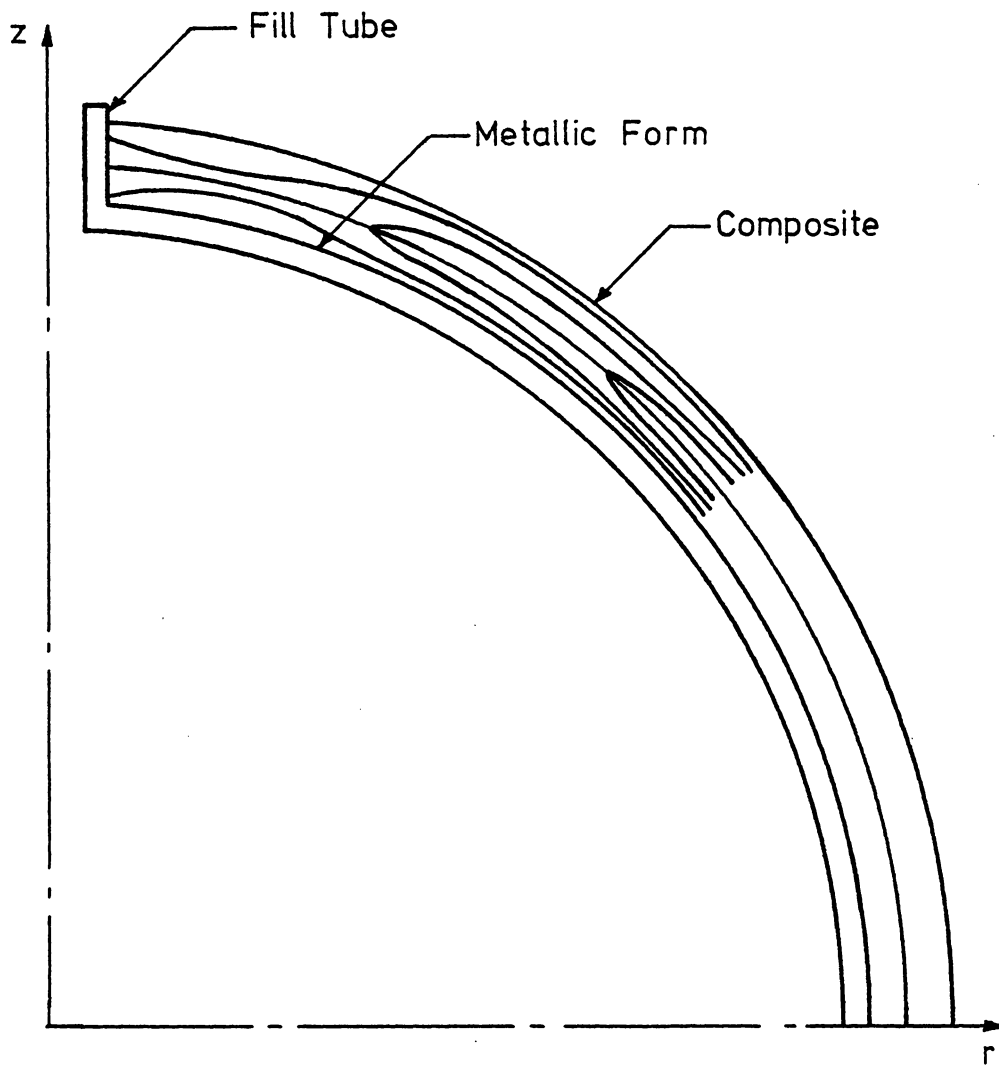
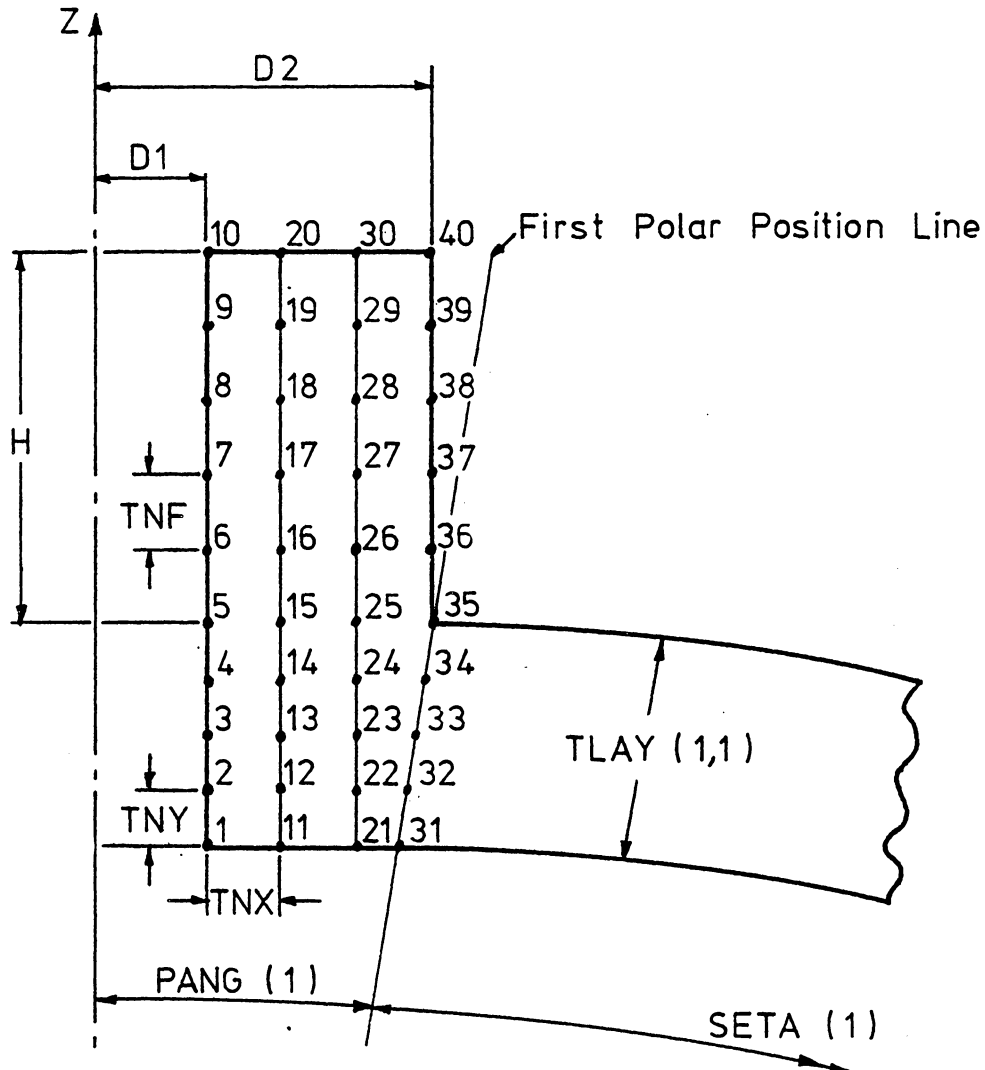


Figure 6. Coordinate System of the Mesh Generator for the Process Model.

generates a fixed number of nodes along each radial line and ensures that nodes fall on the boundaries of each layer in the composite. A constant number of nodes in the radial direction with sequential node numbering will keep the bandwidth of the structural stiffness matrix used in the finite element analysis minimized and constant for computational efficiency. The actual node placement or generation is separated into two segments, one for the fill tube and one for the rest of the model.

The generation of nodes throughout the fill tube requires the following data to be input; the inside and outside diameters of the fill tube, the height of the fill tube, the inside radius of the spherical form, the thickness of the spherical form, the required number of elements through the fill tube wall, the required number of elements along the fill tube, the required number of elements through the spherical form wall and finally the starting polar angle for the composite nodal generation. The base of the fill tube is assumed to be flat joining the spherical form at the first polar position as shown in Fig. 7. The first polar position is chosen so that it passes through the intersection of the outside diameter of the fill tube and the outside of the spherical form.

Nodes are created throughout the fill tube starting on the base and at the inside diameter (node number 1). The



Where

$$TNY = TLAY(1,1) \times \cos[PANG(1)] / NF$$

$$TNX = (D2 - D1) / (2 \times NH)$$

$$TNF = H / NV$$

NF = Number of elements through spherical form

NV = Number of elements up fill tube

NH = Number of elements across fill tube

Figure 7. An Example of Node Point Placement for the Fill Tube.

nodes are created by moving up the inner surface of the fill tube and numbering in sequence. The node spacing is shown in Fig. 7. When the top of the fill tube is reached the nodes are then created on a line parallel to the inner surface starting at the base of the fill tube and spaced over a distance  $TNX$ . This continues to the outside diameter. Here a slight modification occurs in the placement of the nodes. The first few nodes are placed on the first polar line until the intersection with the outside diameter is reached, then they are placed up the outside of the fill tube. This intersection of the outside diameter and the first polar line will be the starting point for the rest of the node generation. Flags are set to identify this point and the inner node on this polar line as the bounds of the spherical form at the first polar position.

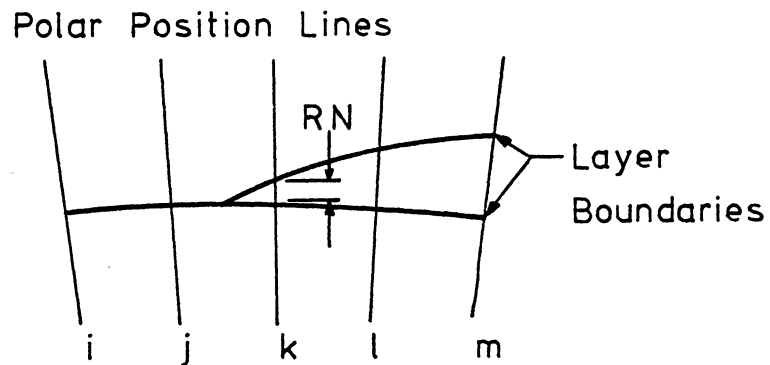
The generation of nodes throughout the rest of the model treats the spherical form as one of the layers in all aspects except in the input of layer thickness and fiber angles. The thickness of the spherical form is constant at  $TLAY(1,1)$  and the fiber angles at all nodes within the spherical form are set to zero as the fiber angle has no significance in the form.

This part of the program requires the input of the total number of elements to be generated through all the fiber layers and the number of polar positions to be used. The

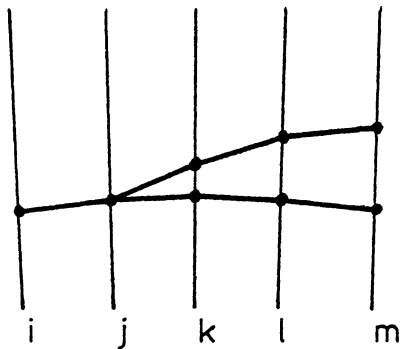


program then loops over all the polar positions and at each polar position the following information is read in; 1) the polar angle and the total thickness of all the fiber layers, and 2) each layer thickness and fiber angle at the start and finish of the band. The nodes are spaced along the radial lines such that a node is placed at every layer boundary. The number of nodes placed within any one layer is dependent upon the proportion of that layer thickness to total composite thickness. The start and finish nodes at each polar position identifying layer boundaries are flagged for use in the element formulation part of the program.

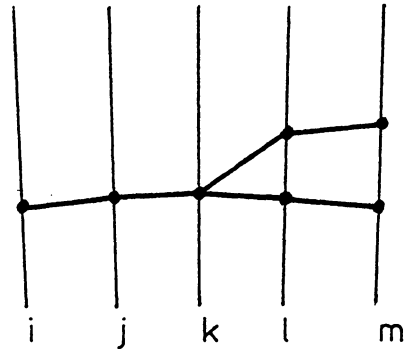
All layers must have at least one node space or there will be no element generated in that layer. There is one exception to this rule, that occurs at the leading edge of a layer's spherical coverage. At the leading edge of coverage it is very unlikely that it will start exactly on a polar position line as shown in Fig. 8. The program decides whether to create a node space or not by the actual thickness of the layer on the specified polar line. If the actual layer thickness is greater than one quarter the thickness of the nominal node space a node space will be generated. The nominal node space is the total composite thickness divided by the required number of elements. If no node space is created the start and finish flags for that layer will be the same.



a) Actual relationship between polar position lines and layer boundaries.



If  $RN > NT/4$



If  $RN < NT/4$

Where  $NT$  - Total composite thickness divided by the number of elements through the composite.

b) Two possible modeling solutions to a layer starting.

Figure 8. Start of a Layer.

The nodes are numbered starting on the first polar line in the first layer. The numbering then moves radially outwards along the polar line until the outer surface is reached. The next node to be numbered is on the second polar line at the inner surface of the spherical form. The numbering then moves radially outward to the outer surface and then back to the inner surface on the next polar position as shown in an example in Fig. 9. This is continued for all polar lines.

Each node placed within the composite is assigned a fiber angle, BETA. The fiber angle of the inner and outer surfaces of a layer are known from the thickness calculation program, NTHICK. The nodes on layer boundaries are assigned two fiber angles, one for each of the two layers meeting at that boundary. The nodes between layer boundaries are assigned fiber angles using a linear distribution from layer boundary to layer boundary. The nodes within the fill tube and the spherical form are assigned zero fiber angles.

### 2.3.2 Element Generation

The element generation part of the program has one constraint. It is that no element may cross a band set layer boundary. The element generator generates two types of elements; corner-noded quadrilaterals and triangles. The actual element generation is separated into two parts. The first part is for the fill tube and the second part is for

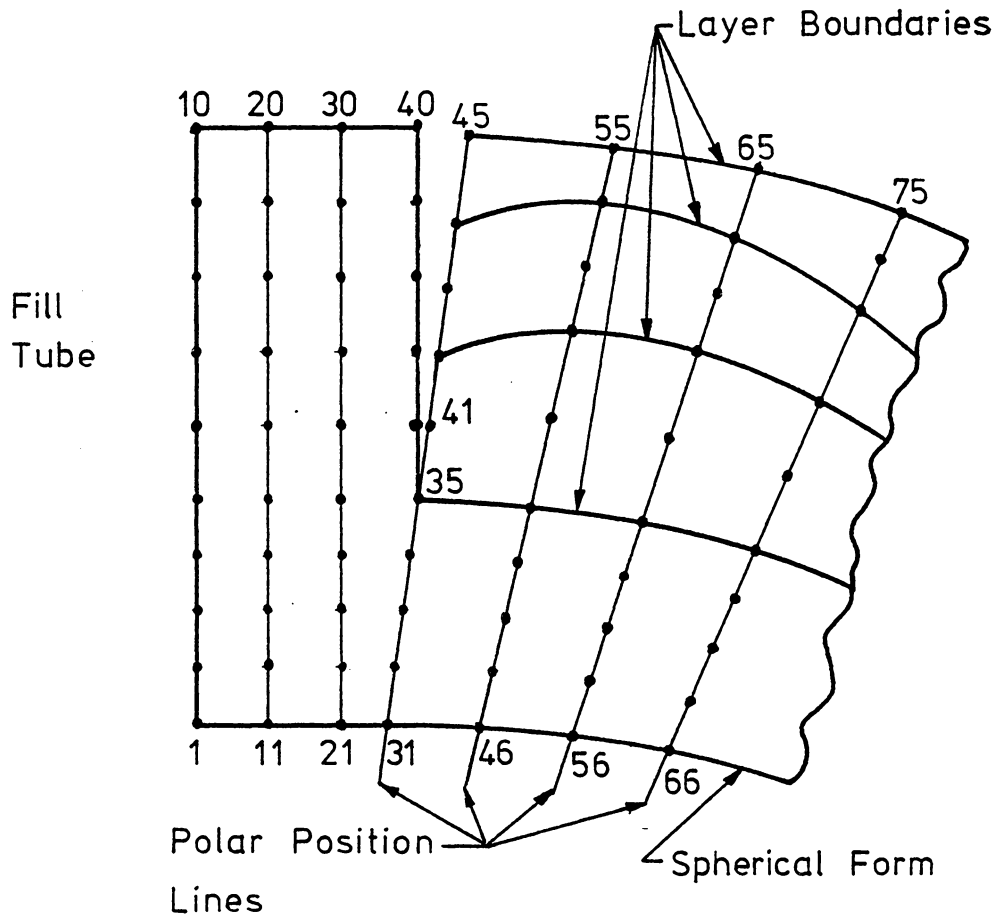


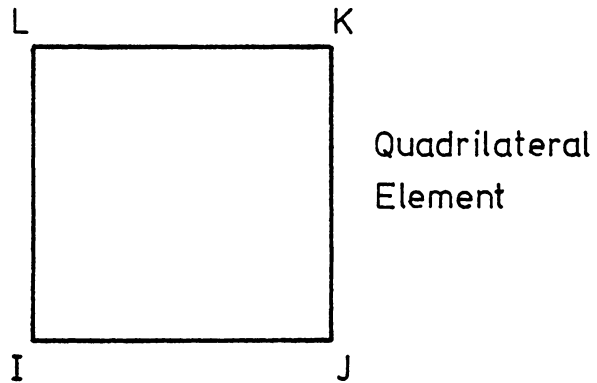
Figure 9. An Example of Node Point Placement for the Composite Layers.

the rest of the model.

The elements in the fill tube and form are all quadrilaterals. The node number sequence of all elements starts with the lower left-hand corner node and connects four nodes in a counterclockwise direction to create the quadrilateral element.

The elements within the fill tube are created in columns parallel to the polar axis starting at the inner diameter of the fill tube. The columns of elements are created outwards to the outer diameter of the fill tube. The first element in the fill tube begins by using the inner surface vertical line of nodes and the next vertical line of nodes. The element definition is illustrated in Fig. 10. The first element uses the first two nodes on each vertical line. The elements are created moving outwards along these two lines of nodes. This continues until the whole fill tube is covered with quadrilateral elements. The elements are numbered as they are created outward in columns. All the elements within the fill tube are assigned zero BETA angles (fiber orientation angles) and 90 degree SETA angles (polar position angles). The SETA angle is defined to be 90 degrees minus the polar angle, PANG, as shown in Fig. 7.

The rest of the elements cover the remaining spherical form and the fiber composite part of the model. The elements generated will mainly be quadrilaterals with



9	18	27
8	17	26
7	16	25
6	15	24
5	14	23
4	13	22
3	12	21
2	11	20
1	10	19

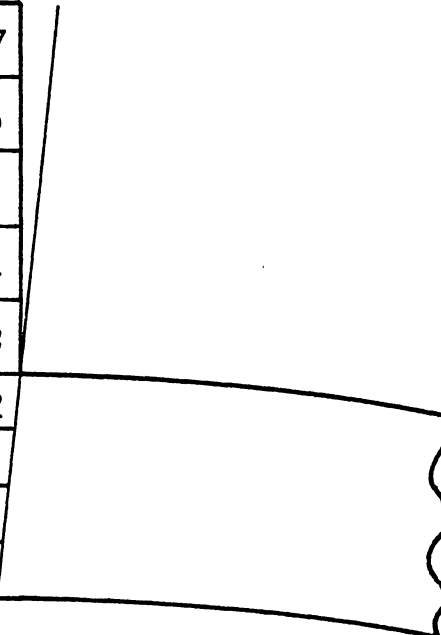


Figure 10. An Example of Element Numbering for the Fill Tube.

triangular elements being used where transitions are necessary. Transitional elements are necessary to allow for the changes in a layer thickness by changing the number of elements from polar position to polar position. The triangular elements are collapsed quadrilateral elements. Element generation is carried out layer by layer. The generation within a layer is by columns of element along polar position lines moving from the fill tube to the equator.

The node numbering sequence is along radial lines with the same number of nodes on each radial line. This ensures that the band width of the assembled structural matrix is as small as possible. The element numbering sequence is carried out in the same order as the element generation sequence for each layer, then layer by layer. While this element numbering sequence simplifies the turning on and off of elements layer by layer using the IOFFON option, it creates a very large wavefront (bandwidth) in a finite element program using a wavefront equation solver. Thus, a program using a wavefront solver is not suitable in this application.

The elements are created between two consecutive polar position lines of nodes as shown in Fig. 11. The program first checks to see if any triangular transition elements are required in this element column of the current layer.

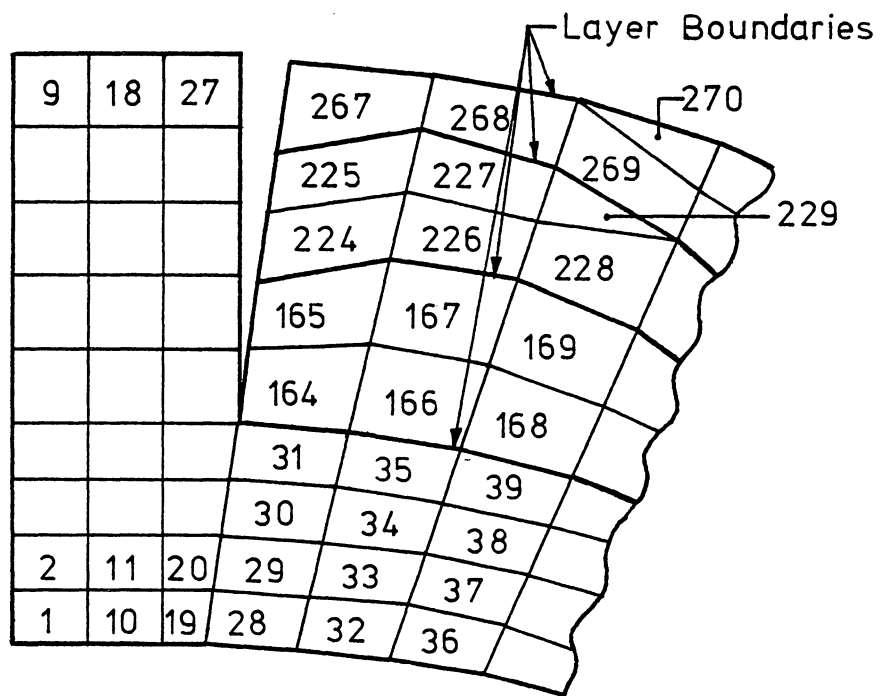
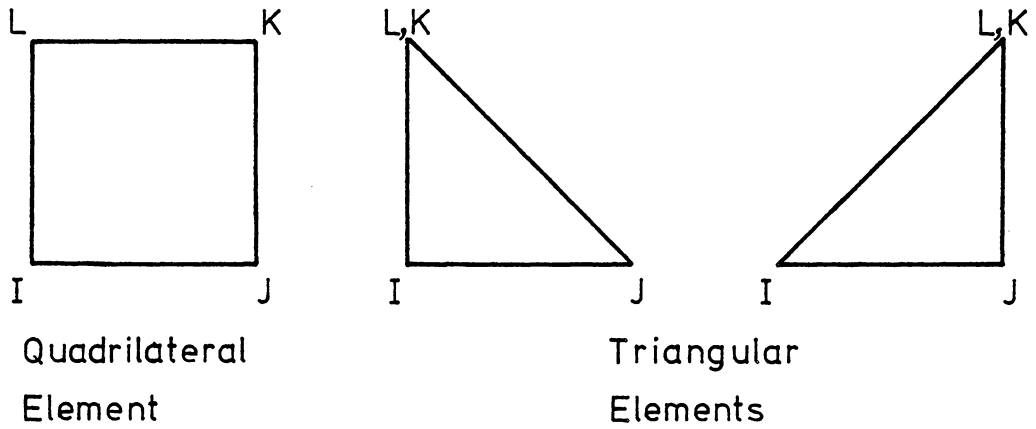


Figure 11. An Example of Element Numbering for the Composite Layers.



The check for triangular elements is made by comparing the node number difference between the start and finish flags of the layer along the two polar lines. If the difference is zero no triangular elements are required at this position. A quadrilateral element is formed by letting corners I and J take on the nodal point numbers of the start flags of the first and second polar lines, respectively. Quadrilateral corners K and L take on nodal point numbers corresponding to J+1 and I+1 positions, respectively. The second element is created by letting all node numbers increment by one. This continues until the finish flags for the layer are reached. For the last element in the layer's column L corresponds to the finish flag of the first polar line and K corresponds to the finish flag of the second polar line. When the finish flags have been reached, the element generation moves over one column to work along the second and third polar lines. Again the program checks to see if any triangular elements are required. If not it proceeds as before.

If triangular elements are required, the procedure begins in the same manner by working up along two polar lines. When one of the corners K or L reaches a finish flag the other corner has not reached a finish flag, therefore one or more triangular elements must be added until both finish flags are reached. Two forms of the triangular elements are possible depending on which corner first encounters a finish flag. The following assumes that corner K (along the right

side node line) encounters a finish flag first. The next element is formed by incrementing all nodes by one except for corner K which is set equal to L to form the triangular element. The program then checks to see if node L has reached its finish flag. If so it proceeds to the next element column, and if not it creates another triangular element. The second triangular element is formed by J remaining the same and incrementing other node values by one. The program again checks to see if L has reached its finish flag, and if not additional triangular elements are generated until L reaches the finish flag.

Similar to the discussion above, if corner L had reached the finish flag first the procedure is very similar, but with I remaining stationary instead of J.

The program creates both quadrilateral and triangular elements from the first polar position to the last polar position layer by layer. Each element is assigned both a fiber angle, BETA, and a polar angle, SETA. The fiber angle is the average of the fiber angles of its four nodes and the polar angle is the average of the angles for the two polar lines that form the element sides.

## 2.4 Fiber Length Calculation

The mesh generator program performs one more task, that is, it calculates the fiber length in each element. This

length will be used in the finite element analysis program, COMSPH, to calculate the average fiber path strain within a layer.

The length of the fibers passing through an element is found by dividing the element volume by the cross-sectional area of all the bands in that layer. The element volume is its cross-sectional area in the r-z plane times its mean circumference about the polar axis. The cross-sectional area of all the bands in that layer are found by summing all the elemental volumes in the layer and dividing by the band-path length. The band-path length is calculated by averaging the spherical radius for a layer, then the length is simply the circumference using that spherical radius.

It is possible that for a few elements near the fill tube that all of the bands within a layer might not pass through these elements. This is most likely to occur when the width of the elements near the fill tube are less than the band width. If this is the case, proportionalizing must be done to correct the fiber lengths. The ratio of element width (arc length between two polar lines) to band width times the fiber length calculated as above will give the corrected fiber lengths for those elements.

## Chapter 3

### Finite Element Program Development

#### 3.1 Introduction

The solution of continuum mechanics problems is obtained by mathematically solving the governing differential equations. The exact solution, except for the most simple cases, cannot be found in general. Therefore, the solution to these continuum problems must make use of a numerical method that converges to the exact solution in the limit. All numerical methods involve some approximations to obtain a solution. The approximations fall basically into two groups; the first is to make an approximation of the governing differential equations, and the second is to approximate the continuum. The finite element method falls into the second group as it approximates the continuum.

#### 3.2 Finite Element Approach

There are several approaches used in solving a continuum problem by the finite element method. The majority of finite element approaches are based on the principle of virtual work (or its equivalent the principle of minimum potential energy). In this displacement approach the approximation of the continuous system is made as follows. The continuum is divided into a finite number of sections or elements. The elements are assumed to be interconnected at

a discrete number of nodal points situated on their boundaries. The displacement of these nodal points are the unknown parameters of the problem. A set of functions are chosen to define uniquely the state of displacement within each element in terms of its nodal displacements. The displacement functions now define uniquely the state of strain within an element in terms of nodal displacements. The stress state throughout the element can be found from these strains, plus any initial strains using the constitutive properties of the material. If a degree of freedom is defined to be a displacement or rotation of a node, then an element with  $n$  degrees of freedom will have  $n$  equations which relate node forces and displacements through stiffness coefficients.

$$\begin{array}{rcl}
 K_{11}d_1 + K_{12}d_2 + \dots + K_{1n}d_n & = & F_1 \\
 K_{21}d_1 + K_{22}d_2 + \dots + K_{2n}d_n & = & F_2 \\
 \vdots & & \vdots \\
 K_{n1}d_1 + K_{n2}d_2 + \dots + K_{nn}d_n & = & F_n
 \end{array} \tag{3.2-1}$$

where  $d_i$  -  $i^{\text{th}}$  degree of freedom

$F_i$  -  $i^{\text{th}}$  force or moment applied to the element

$K_{ij}$  - stiffness coefficients

The equations of 3.2-1 are gathered into matrix form to give the relationship

$$[K]\{d\} = \{F\} \tag{3.2-2}$$

where  $[K]$  - element stiffness matrix

$\{d\}$  - vector of nodal displacement

$\{F\}$  - vector of element nodal forces

In this approach some approximations are involved. One, the chosen displacement functions will not necessarily, but usually do, satisfy the requirements of displacement continuity between adjacent elements. Thus, the compatibility condition on such lines may be violated. Two, by concentrating forces at nodes only, equilibrium conditions are satisfied in the overall sense only. Some local violations of equilibrium conditions within each element and on its boundaries may arise. The choice of element shape and the form of the displacement function will affect the degree of approximation for specific cases.

The chosen displacement function for the element is a polynomial in  $\xi$  and  $\eta$  as given in equation 3.2-3 and described in the element development section 3.3. The displacement function is continuous within the element, thus compatibility is satisfied within the element.

$$\begin{aligned} u &= a_1 + a_2\xi + a_3\eta + a_4\xi\eta \\ v &= a_5 + a_6\xi + a_7\eta + a_8\xi\eta \end{aligned} \tag{3.2-3}$$

Since the element is square in the  $\xi, \eta$  coordinate system, for the displacement function given in equation 3.2-3 compatibility is also satisfied along interelement

boundaries as the element sides remain straight when the element is deformed. The chosen displacement function satisfies the equations of equilibrium at the nodes of the element and within the element, but not along interelement boundaries.

The development of the finite element program COMSPH is based on the finite element program STAP as taken from reference 3. The axisymmetric quadrilateral isoparametric element was then added to the program together with the capacity for turning elements off or on as required to obtain incremental fabrication modeling. Material property transformation is necessary to obtain material properties in global coordinates from orthotropic properties at an arbitrary fiber orientation. The capacity of calculating nodal loads from initial fiber stresses or winding tension needs to be added. The output of stresses and strains is required for every element in both global and local coordinates, layer-by-layer and accumulated. The final modification to the program is to calculate the average fiber band path strain.

A brief outline of the finite element program COMSPH follows:

The heading and various control information are input.

The externally applied nodal loads are input.

The element type is input.

Temporary storage is assigned based on element type.

Nodal point and element data are input.

Nodal point and element data are stored.

Element stiffness is calculated using the necessary  
material property transformations.

Element stiffness is reduced for elements not turned ON.

Nodal loads are calculated from initial stresses.

Structural stiffness matrix is assembled for this load  
step.

Structural stiffness matrix is decomposed.

The system of equations are solved.

Nodal displacements are output.

Element strains are calculated.

Element stresses in global coordinates are output.

Strains are transformed from global to fiber coordinates.

Element stresses in fiber coordinates are output.

Geometry is updated.

Accumulated stresses in both global and fiber coordinates  
are output.

Proceeds to next load step.

### 3.3 Element Development

The element chosen to be used in the analysis of the spheres is an axisymmetric, four-noded, two-dimensional, isoparametric element capable of handling both isotropic and orthotropic materials. The isoparametric element maps the



arbitrarily (within reasonable bounds) shaped quadrilateral in the  $r$ - $z$  plane of the axisymmetric coordinates  $(r, z, t)$  to a square element in a natural coordinate system  $(\xi, \eta)$  as shown in Fig. 12. The mapping parameters are called shape functions. When the mapping parameters are the same for the geometry mapping as for the displacement mapping of displacements within the element then the element is called isoparametric. The shape functions are defined in the natural coordinate system and represent surfaces defined over the isoparametric element such that each shape function has unit value at one node and zero at all other node points. The shape functions in natural coordinates are

$$\begin{aligned} N_1 &= \frac{1}{4}(1 - \xi)(1 - \eta) & N_3 &= \frac{1}{4}(1 + \xi)(1 + \eta) \\ N_2 &= \frac{1}{4}(1 + \xi)(1 - \eta) & N_4 &= \frac{1}{4}(1 - \xi)(1 + \eta) \end{aligned} \quad (3.3-1)$$

The relationship between  $r$ - $z$  coordinates and natural coordinates are

$$r(\xi, \eta) = \sum_{i=1}^4 N_i r_i \quad (3.3-2)$$

$$z(\xi, \eta) = \sum_{i=1}^4 N_i z_i$$

where  $r(\xi, \eta), z(\xi, \eta)$  -  $r$ - $z$  coordinates of any point  
located in natural coordinates  
 $r_i, z_i$  - node point coordinates in  $r$ - $z$   
coordinates

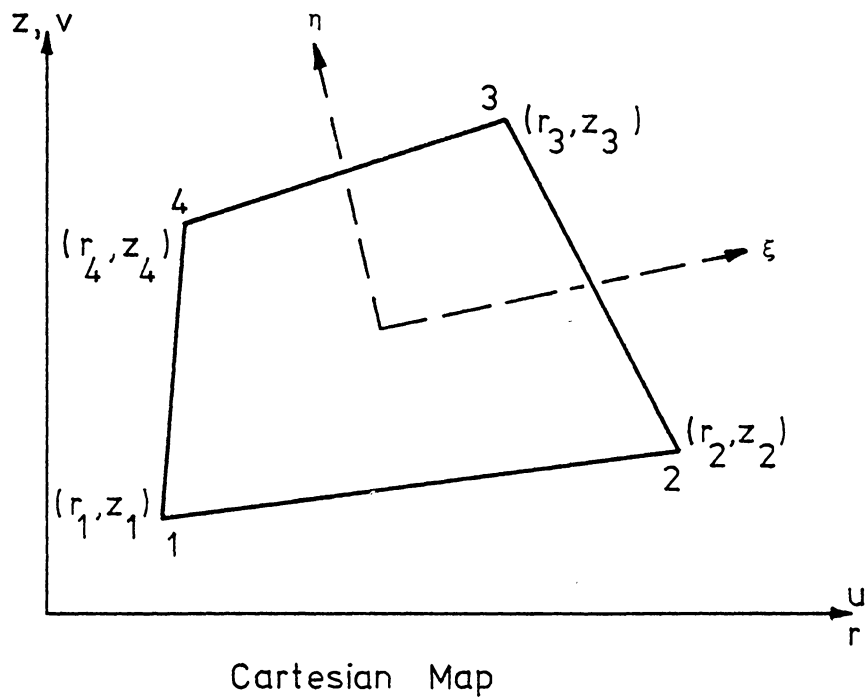
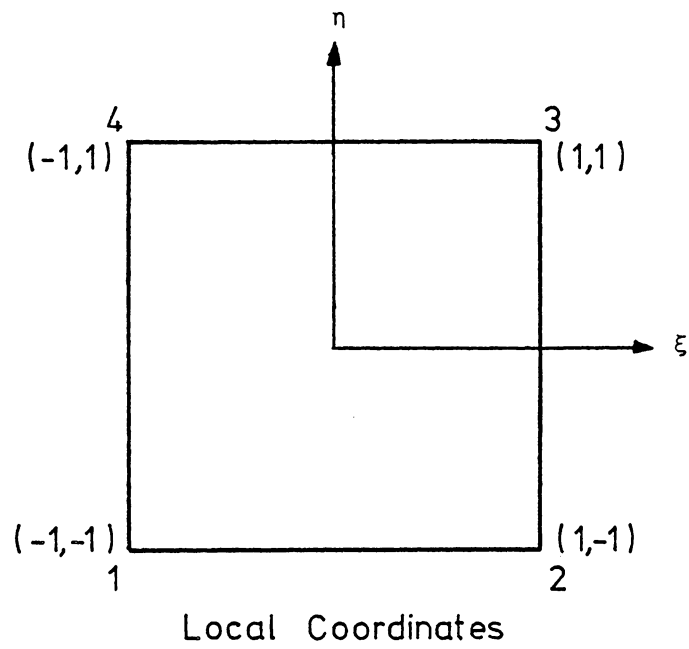


Figure 12. Mapping of the Quadrilateral Element into  $r$ - $z$  Space.

The relationship for the displacements between the two coordinate systems are similarly stated

$$\begin{aligned} u(\xi, \eta) &= \sum_{i=1}^4 N_i u_i \\ v(\xi, \eta) &= \sum_{i=1}^4 N_i v_i \end{aligned} \quad (3.3-3)$$

where  $u(\xi, \eta)$ ,  $v(\xi, \eta)$  - displacements of any point located  
in natural coordinates

$u_i$ ,  $v_i$  - node point displacements in  
cartesian coordinates

Expressed in matrix form

$$\begin{Bmatrix} u(\xi, \eta) \\ v(\xi, \eta) \end{Bmatrix} = \begin{bmatrix} N_1 & 0 & N_2 & 0 & N_3 & 0 & N_4 & 0 \\ 0 & N_1 & 0 & N_2 & 0 & N_3 & 0 & N_4 \end{bmatrix} \begin{Bmatrix} u_1 \\ v_1 \\ u_2 \\ v_2 \\ u_3 \\ v_3 \\ u_4 \\ v_4 \end{Bmatrix} \quad (3.3-4)$$

or

$$\{u\} = [N]\{d\} \quad (3.3-5)$$

where  $\{u\}$  - vector of displacement components in the  
element field

$[N]$  - matrix of shape functions

$\{d\}$  - vector of nodal displacements

Using the minimum potential energy finite element formulation the potential energy for an element in this system neglecting initial stresses and strains is

$$I^e = \frac{1}{2} \int_{vol} \sigma_{ij} \epsilon_{ij} dvol \quad (3.3-6)$$

where  $I^e$  - potential energy of element

$\sigma_{ij}$  - stress tensor

$\epsilon_{ij}$  - strain tensor

$vol$  - volume of the element

or in matrix form

$$I^e = \frac{1}{2} \int_{vol} \{\sigma\}^t \{\epsilon\} dvol \quad (3.3-7)$$

where  $\{\sigma\}^t$  - transposed matrix form of the stress tensor

$\{\epsilon\}$  - matrix form of the strain tensor

The stress tensor can be replaced by using the stress-strain relationship for orthotropic (or isotropic) materials and the strain tensor

$$\{\sigma\} = [D] \{\epsilon\} \quad (3.3-8)$$

where  $[D]$  - stress-strain relationship matrix.

And then

$$I^e = \frac{1}{2} \int_{vol} \{\epsilon\}^t [D] \{\epsilon\} dvol \quad (3.3-9)$$

where  $\{\epsilon\}^t$  - transposed matrix form of the strain tensor.

The stress-strain relationship for the axisymmetric case is

$$[D] = \frac{1}{Div} \begin{bmatrix} E_r(1-\nu_{zt}\nu_{tz}) & E_z(\nu_{rz}+\nu_{rt}+\nu_{tz}) & E_t(\nu_{rt}+\nu_{rz}\nu_{zt}) & 0 \\ & E_z(1-\nu_{rt}\nu_{tr}) & E_t(\nu_{zt}+\nu_{zr}\nu_{rt}) & 0 \\ & & E_t(1-\nu_{rz}\nu_{zr}) & 0 \\ & & & G_{rz} \end{bmatrix} \quad (3.3-10)$$

where  $Div = (1 - \nu_{rz}\nu_{zr} - \nu_{zt}\nu_{tz} - \nu_{tr}\nu_{rt} - 2\nu_{rz}\nu_{zt}\nu_{tr})$

and

$E_r$  - Young's modulus in the radial (r) direction.

$E_z$  - Young's modulus in the axial (z) direction.

$E_t$  - Young's modulus in the tangential (t) direction.

$G_{rz}$  - Modulus of rigidity between the r and z directions.

$\nu_{zt}$  - Poisson's ratio of t strain to z strain for a z load

$\nu_{rz}$  - Poisson's ratio of z strain to r strain for an r load

$\nu_{rt}$  - Poisson's ratio of t strain to r strain for an r load

$\nu_{tz}$  - Poisson's ratio of z strain to t strain for a t load

$\nu_{tr}$  - Poisson's ratio of r strain to t strain for a t load

$\nu_{zr}$  - Poisson's ratio of r strain to z strain for a z load.

The strain tensor in terms of the displacements is

$$\{\epsilon\} = \begin{Bmatrix} \epsilon_r \\ \epsilon_z \\ \epsilon_t \\ \epsilon_{zr} \end{Bmatrix} = \begin{Bmatrix} \partial u / \partial r \\ \partial v / \partial z \\ u/r \\ \partial u / \partial z + \partial v / \partial r \end{Bmatrix} = \begin{bmatrix} \partial / \partial r & 0 \\ 0 & \partial / \partial z \\ 1/r & 0 \\ \partial / \partial z & \partial / \partial r \end{bmatrix} \begin{Bmatrix} u \\ v \end{Bmatrix} \quad (3.3-11)$$

where  $r$  - radial coordinate

$\epsilon_r$  - radial strain

$\epsilon_z$  - axial strain

$\epsilon_t$  - hoop/tangential strain

$\epsilon_{rz}$  - transverse shear strain

The relationship between the derivatives in the natural coordinate system and the derivatives in the r-z coordinate system are

$$\begin{Bmatrix} \partial / \partial \xi \\ \partial / \partial \eta \end{Bmatrix} = \begin{bmatrix} \partial r / \partial \xi & \partial z / \partial \xi \\ \partial r / \partial \eta & \partial z / \partial \eta \end{bmatrix} \begin{Bmatrix} \partial / \partial r \\ \partial / \partial z \end{Bmatrix} = [J] \begin{Bmatrix} \partial / \partial r \\ \partial / \partial z \end{Bmatrix} \quad (3.3-12)$$

Where  $[J]$  is called the Jacobian matrix.  $[J]$  can be written in terms of the shape functions and the r-z node point

coordinates as

$$[J] = \begin{bmatrix} \sum_{i=1}^4 (\partial N_i / \partial \xi) r_i & \sum_{i=1}^4 (\partial N_i / \partial \xi) z_i \\ \sum_{i=1}^4 (\partial N_i / \partial \eta) r_i & \sum_{i=1}^4 (\partial N_i / \partial \eta) z_i \end{bmatrix} \quad (3.3-13)$$

Taking the inverse

$$\begin{Bmatrix} \partial / \partial r \\ \partial / \partial z \end{Bmatrix} = [J]^{-1} \begin{Bmatrix} \partial / \partial \xi \\ \partial / \partial \eta \end{Bmatrix} \quad (3.3-14)$$

where

$$[J]^{-1} = \begin{bmatrix} J_{11}^* & J_{12}^* \\ J_{21}^* & J_{22}^* \end{bmatrix} \quad (3.3-15)$$

is called the inverse Jacobian matrix.

Rewriting the strain tensor in natural coordinates

$$\begin{aligned} \partial u / \partial r &= J_{11}^* \partial u / \partial \xi + J_{12}^* \partial u / \partial \eta \\ \partial v / \partial z &= J_{21}^* \partial v / \partial \xi + J_{22}^* \partial v / \partial \eta \\ \partial u / \partial z &= J_{21}^* \partial u / \partial \xi + J_{22}^* \partial u / \partial \eta \\ \partial v / \partial r &= J_{11}^* \partial v / \partial \xi + J_{12}^* \partial v / \partial \eta \end{aligned} \quad (3.3-16)$$

or in matrix form

$$\{\epsilon\} = \begin{bmatrix} (J_{11}^* \partial/\partial \xi + J_{12}^* \partial/\partial \eta) & 0 \\ 0 & (J_{21}^* \partial/\partial \xi + J_{22}^* \partial/\partial \eta) \\ 1/r & 0 \\ (J_{21}^* \partial/\partial \xi + J_{22}^* \partial/\partial \eta) & (J_{11}^* \partial/\partial \xi + J_{12}^* \partial/\partial \eta) \end{bmatrix} \begin{Bmatrix} u \\ v \end{Bmatrix} \quad (3.3-17)$$

using equation 3.3-5 the element strain is

$$\{\epsilon\} = [B]\{d\} \quad (3.3-18)$$

where  $[B]$  - matrix of strain shape functions.

The potential energy for the element becomes

$$I^e = \frac{1}{2} \int_{vol} \{d\}^t [B]^t [D] [B] \{d\} dvol \quad (3.3-19)$$

Then summing over all the elements, the potential energy for the whole structure is

$$I = \sum_{n=1}^m \frac{1}{2} \int_{vol} \{d\}^t [B]^t [D] [B] \{d\} dvol + P.E. \quad (3.3-20)$$

where  $m$  - total number of elements in the structure

P.E. - potential of external loads

Taking the derivative with respect to  $\{d\}$  of the potential energy and equating it to zero

$$\delta I = 0 = \sum_{n=1}^m \left[ \int_{vol} [B]^t [D] [B] dvol \right] \{d\} + \{F\} \quad (3.3-21)$$



where  $\{F\}$  - vector of external loads

The volume integral can be replaced by  $r d\theta dr dz$  which can also be replaced by  $r(\det|J|)d\theta d\xi d\eta$  in natural coordinates.

$$\sum_{n=1}^m \left[ \int_0^1 \int_{-1}^1 \int_{-1}^1 [B]^t [D] [B] r(\det|J|) d\theta d\xi d\eta \right] \{d\} = -\{F\} \quad (3.3-22)$$

Assuming one radian of arc for the tangential integration

$$\sum_{n=1}^m \left[ \int_{-1}^1 \int_{-1}^1 [B]^t [D] [B] r(\det|J|) d\xi d\eta \right] \{d\} = -\{F\} \quad (3.3-23)$$

We define the stiffness matrix to be

$$[K^e] = \int_{-1}^1 \int_{-1}^1 [B]^t [D] [B] r(\det|J|) d\xi d\eta \quad (3.3-24)$$

The integral is a complicated polynomial in  $\xi$  and  $\eta$  and cannot be readily evaluated explicitly. Instead, the element matrices are evaluated using numerical integration techniques. The numerical technique chosen for the quadrilateral elements was a two point Gauss Quadrature.

Gauss Quadrature evaluates the function at sampling points located to achieve the best accuracy and multiplies the value by weighting coefficients to obtain the value of the integral.

In equation form

$$\int_{-1}^1 \int_{-1}^1 f(\xi, \eta) d\xi d\eta = \sum_{i=1}^2 \sum_{j=1}^2 H_i H_j f(\xi_i, \eta_j) \quad (3.3-25)$$

where  $f(\xi, \eta)$  - function to be integrated

$f(\xi_i, \eta_j)$  - value of the function at the sampling  
point.  $i, j = 1, 2$

$H_i$  and  $H_j$  - weighting coefficients at the sampling  
points.  $i, j = 1, 2$

The element can be made to represent a triangular element by allowing any two nodes of the quadrilateral to coincide. Triangular elements formed in this way are like regular triangular elements but with double weighting given to one corner. This means that the element is sensitive to how it is numbered, sometimes called anisotropy. If the node order of the element is permuted from  $i \ j \ k$  to  $k \ i \ j$ , different results would be obtained from the element. The amount of anisotropy can be reduced by reducing the order of the Gauss quadrature for these elements. For the triangular elements formed in this way the order of the Gauss Quadrature was reduced to single point integration. This reduces the element anisotropy with respect to its node number sequence. Some triangular elements are necessary where the thickness of a fiber layer changes quickly to allow smoother approximations of the boundaries.

### 3.4 Material Properties Transformation

The material properties of the fiber composite are orthotropic, with the principal directions along and perpendicular to the fiber path. The sphere, being wound to a set pattern, has fibers in many directions. These directions are known from the winding pattern for all elements.

The element stiffness is calculated in the r-z-t or global coordinate system for all elements of the model. This means that the material properties of the composite will have to be transformed to the r-z-t or global coordinate system from the prescribed fiber orientation as shown in Fig. 13. The fiber coordinate system, 1-2-3 has the 1 axis aligned along the fibers with the 2 axis being in the band plane and perpendicular to 1. The 3 axis is then in the outward radial direction of the sphere to complete the right-hand coordinate system.

The transformation from the fiber or 1-2-3 coordinate system to the r-z-t or global coordinate system requires two fourth order tensor transformations. The transformation matrix is shown in Fig. 14 and was obtained from reference 24. The fourth order transformation is obtained by post multiplying the material property matrix by a second order transformation matrix and premultiplying by the transpose of

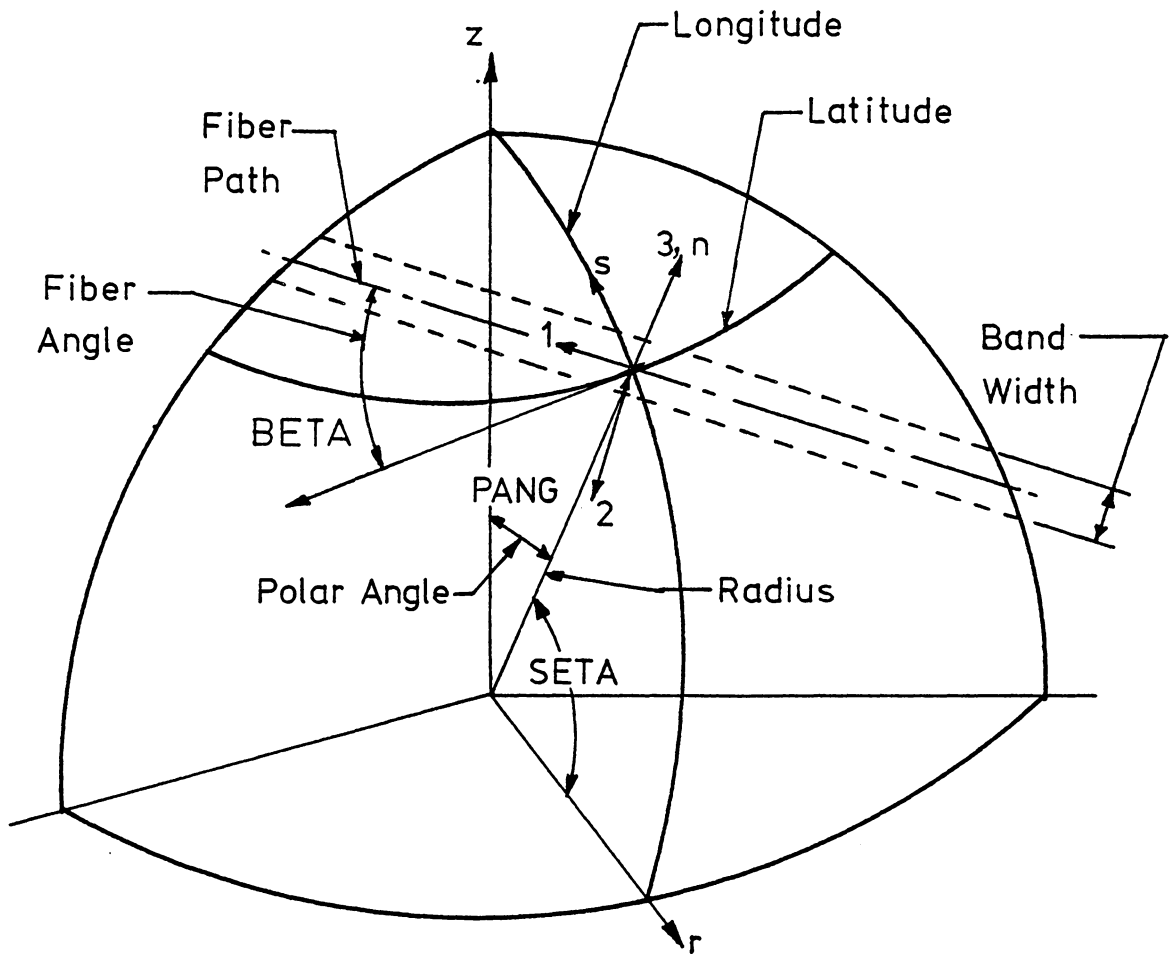


Figure 13. Three Dimensional View of the Transformation Angles BETA and SETA.

$$[T_m] = \begin{bmatrix} N^2 & M^2 & 0 & 0 & 0 & -2MN \\ M^2 & N^2 & 0 & 0 & 0 & 2MN \\ 0 & 0 & 1 & 0 & 0 & 0 \\ 0 & 0 & 0 & N & M & 0 \\ 0 & 0 & 0 & -M & N & 0 \\ MN & -MN & 0 & 0 & 0 & M^2 - N^2 \end{bmatrix}$$

where  $M$  - sine of the rotation angle between the 1-axis and the 1'-axis.

$N$  - cosine of the rotation angle between the 1-axis and the 1'-axis.

where the transformation is from the unprimed to the primed coordinate system.

Figure 14. Material Property Transformation Matrix.

the second transformation matrix as shown in equation 3.4-1.

$$[D'] = [T_m]^t [D] [T_m] \quad (3.4-1)$$

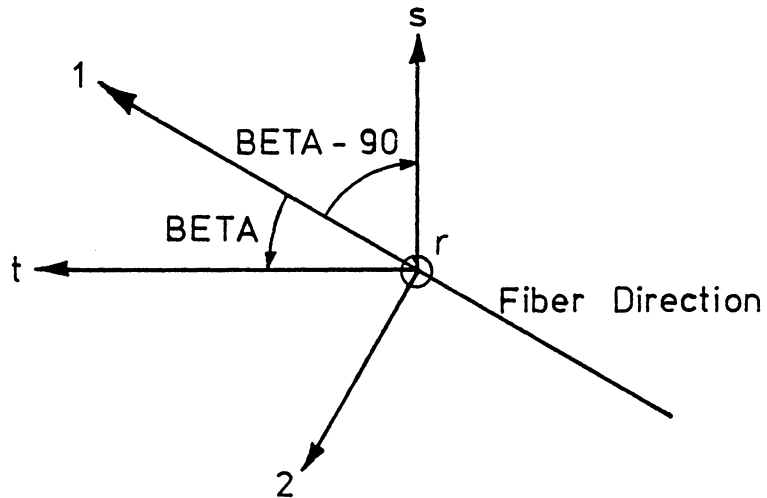
where  $[D]$  - matrix of material properties  
 $[D']$  - matrix of transformed material properties  
 $[T_m]$  - second order transformation matrix  
 $[T_m]^t$  - transposed second order transformation matrix

Figure 15 shows the two transformation angles BETA and SETA between the coordinate systems. The first transformation is a negative rotation about the 3,n axis to the s-t-n coordinate system through the angle (BETA-90). The s-t-n coordinate system has the s axis aligned along a longitudinal line with the t axis being tangent to the latitude line in the band plane. The n axis then coincides with the 3 axis to complete the right hand coordinate system. The order of the s-t-n coordinate system is then permuted to make an n-s-t coordinate system. The second transformation is a negative rotation about the t axis. This negative transformation through the angle SETA gives the material properties in the r-z-t or global coordinate system.

### 3.5 Stress and Strain Computations

Stresses for every element are calculated in both local fiber and global (r,z,t) coordinate systems. The elemental stresses in global coordinates are calculated using equation

BETA View along spherical radius or  $n$  and  $3$  axis.



SETA View in tangential direction along the  $t$  axis.

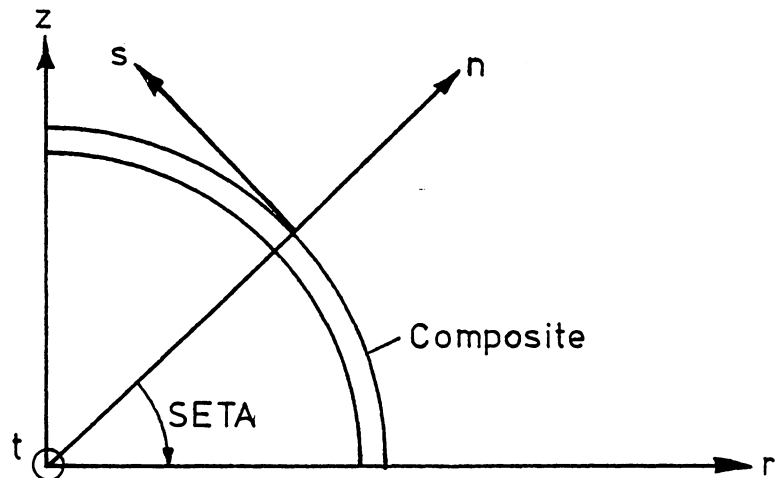


Figure 15. Transformation Angles - BETA and SETA.

3.3-8 on page 44 and equation 3.3-18 on page 48. The stresses are calculated at the four Gauss points and then averaged to give element stresses. The stresses are then added load step-by-load step to give the final accumulated stress of every element in global coordinates.

The output of element stresses in fiber coordinates involves a transformation from global to fiber coordinates. This transformation is carried out on element strains rather than directly on the stresses. Element strains are transformed since the fiber direction within an element is made up of an equal number of + and - orientations due to bands crossing. The bands cross the equator at a set angle as shown in Fig. 4 and each band set gives two layers of coverage at the equator. This means that any point on the sphere has two bands crossing it at opposite angles within every band set as shown in Fig. 16. At this point the strain components in any direction within the two bands must be the same. However, stress components in any direction in the two bands would generally be different. Therefore, transformation of global element stress components would give the average stress for the two bands. This averaged stress of the two bands is not the correct fiber direction stress. The transformation of the element strains yields the correct fiber direction strains. The fiber direction stresses are obtained by premultiplying the fiber direction strains by the material stiffness matrix. These stresses



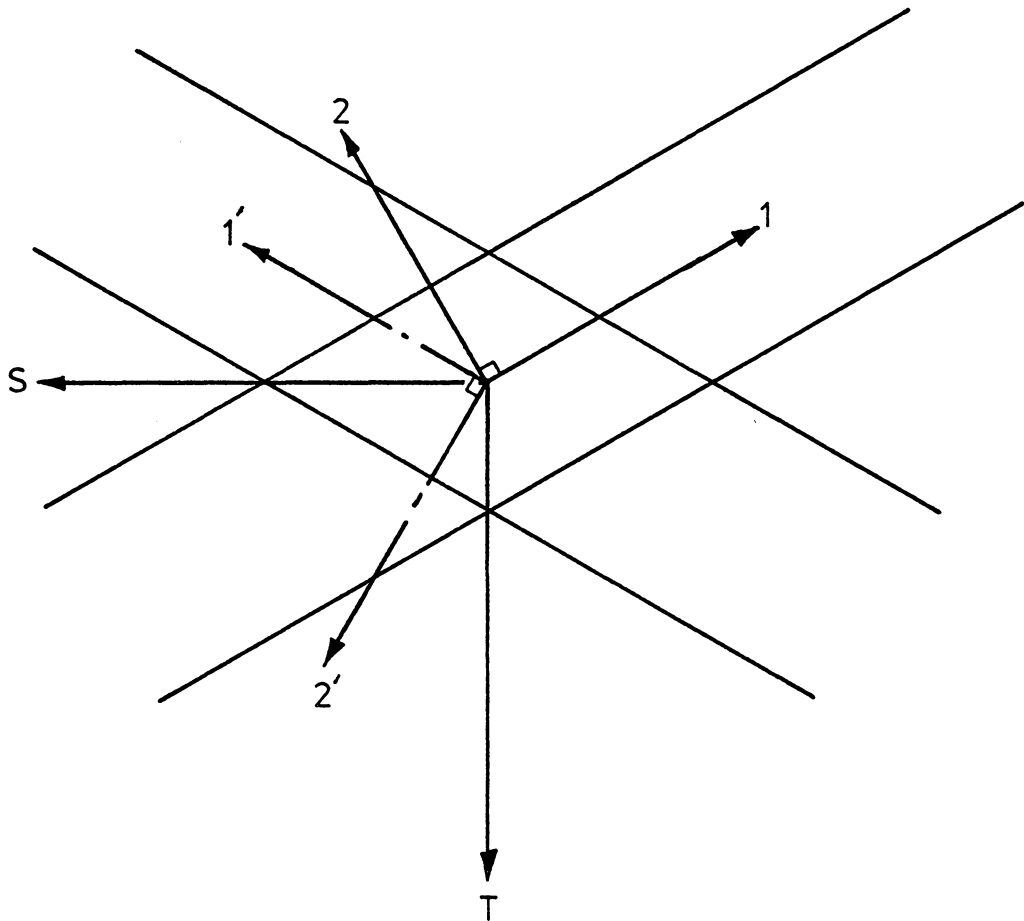


Figure 16. Crossing of Bands within a Layer.

are also added load step-by-load step to give the final accumulated stress of every element in fiber coordinates.

### 3.6 Strain Transformation

Stresses in the fiber coordinate system are required for any strength analysis which must be obtained by strain transformation. The program calculates nodal displacements in axisymmetric coordinates (r,z). These displacements are multiplied by the [B] matrix evaluated at the four Gauss points and averaged to obtain average elemental strains in global or r-z-t coordinates (see equation 3.3-18). The second order transformation matrix is shown in Fig. 17 and the transformation is of the form

$$\{\epsilon'\} = [T_s]\{\epsilon\} \quad (3.6-1)$$

where  $\{\epsilon\}$  - tensor of strains

$\{\epsilon'\}$  - tensor of transformed strains

$[T_s]$  - second order transformation matrix

The transformation from the global or r-z-t coordinate system to the fiber or 1-2-3 coordinate system requires two second order tensor transformations. The transformation matrix is different than that for the material property transformation matrix as the angle rotated through is now positive.

The two transformation angles BETA and SETA between the

$$[T_s] = \begin{bmatrix} M^2 & N^2 & 0 & 0 & 0 & -2MN \\ N^2 & M^2 & 0 & 0 & 0 & 2MN \\ 0 & 0 & 1 & 0 & 0 & 0 \\ 0 & 0 & 0 & M & -N & 0 \\ 0 & 0 & 0 & N & M & 0 \\ -MN & MN & 0 & 0 & 0 & M^2 - N^2 \end{bmatrix}$$

where  $M$  - sine of the rotation angle between the 1-axis and the 1'-axis.

$N$  - cosine of the rotation angle between the 1-axis and the 1'-axis.

where the transformation is from the unprimed to the primed coordinate system.

Figure 17. Strain Transformation Matrix.

coordinate systems are shown in Fig. 15. The first transformation is a positive rotation about the  $t$  axis to the  $n$ - $s$ - $t$  coordinate system through the angle  $(90-\text{BETA})$ . The order of the  $n$ - $s$ - $t$  coordinate system is then permuted to make a  $s$ - $t$ - $n$  coordinate system. The second transformation is a positive rotation about the  $n$  axis to the fiber or 1-2-3 coordinate system.

The element strains are now defined in the fiber coordinate system. The principal material direction stresses are then calculated by premultiplying the strains by the fiber's material property matrix  $[D]$  defined in the 1-2-3 or fiber coordinate system.

### 3.7 Nodal Loads from Initial Stresses

The composite sphere is made by winding the filaments, grouped together in bands, onto the spherical form at a set polar angle. When the required number of bands for that polar angle have been wound onto the sphere one layer of the composite has been formed. Each layer of the composite is formed in the same way, but with different polar angles and different numbers of bands. In this study it is assumed that all the bands in a layer are applied simultaneously and that each composite layer will form a load step in the fabrication process model.

The vector of element nodal forces  $\{F\}$  of equation 3.2-1

can be separated into four integrals; nodal forces due to initial stresses, nodal forces due to initial strains, nodal forces due to body forces, and nodal forces due to surface tractions.

$$\{F\} = \int_{vol} [B]^t \{\sigma_0\} dvol - \int_{vol} [B]^t [D] \{\epsilon_0\} dvol - \int_{vol} [N]^t \{b\} dvol - \int_{area} [N]^t \{t\} darea \quad (3.7-1)$$

where  $\{\sigma_0\}$  - vector of element initial stresses

$\{\epsilon_0\}$  - vector of element initial strains

$\{b\}$  - vector of body forces

$\{t\}$  - vector of surface tractions

$[N]$  - matrix of shape functions

Winding tension is taken as an initial stress in the fiber direction. Then if all other forces are zero the potential energy of the element can be written using equations 3.2-2, 3.3-23, and 3.7-1 as

$$\left[ \int_{vol} [B]^t [D] [B] dvol \right] \{d\} = - \int_{vol} [B]^t \{\sigma_0\} dvol \quad (3.7-2)$$

or

$$\left[ \int_{-1}^1 \int_{-1}^1 [B]^t [D] [B] r(\det|J|) d\xi d\eta \right] \{d\} = - \int_{-1}^1 \int_{-1}^1 [B]^t \{\sigma_0\} r(\det|J|) d\xi d\eta \quad (3.7-3)$$

The nodal loads for each load step are calculated using the right-hand side of equation 3.7-3. The initial stresses are those obtained during the fabrication process, which are assumed to be tension in the fiber direction and equal to the net winding tension used in that layer. Since these initial stresses are in fiber coordinates and the analysis is carried out in the r-z-t coordinate system, the initial stresses of each element must be transformed to the r-z-t coordinate system before the vector of nodal loads is calculated. The transformation matrix is shown in Fig. 18 and the transformation is of the form

$$\{\sigma'_0\} = [T_i]\{\sigma_0\} \quad (3.7-4)$$

where  $\{\sigma_0\}$  - tensor of initial stresses

$\{\sigma'_0\}$  - tensor of transformed initial stresses

$[T_i]$  - second order transformation matrix

The transformation of initial stresses from the 1-2-3 coordinate system to the r-z-t coordinate system is made through the same angles as the material property transformation from the 1-2-3 to the r-z-t system. The only difference being that the initial stresses require second order transformation matrices as opposed to the fourth order required by the material properties. The transformation angles are shown in Fig. 15.

$$[T_i] = \begin{bmatrix} N^2 & M^2 & 0 & 0 & 0 & -2MN \\ M^2 & N^2 & 0 & 0 & 0 & 2MN \\ 0 & 0 & 1 & 0 & 0 & 0 \\ 0 & 0 & 0 & N & M & 0 \\ 0 & 0 & 0 & -M & N & 0 \\ MN & -MN & 0 & 0 & 0 & M^2 - N^2 \end{bmatrix}$$

where  $M$  - sine of the rotation angle between the 1-axis and the 1'-axis.

$N$  - cosine of the rotation angle between the 1-axis and the 1'-axis.

Where the transformation is from the unprimed to the primed coordinate system.

Figure 18. Initial Stress Transformation Matrix.

### 3.8 Element IOFFON Option

An off-on element switch provides for the addition of fabricated layers to the structural model as the process is simulated. The model is initially formed with all the elements that are needed to describe the final configuration. The input data that defines each element by its node connectivity also gives the load step or load case sequence number in which the element is turned on. In any given step of the multistep analysis the elements that are turned on represent the wound layers of material that have been applied at that point in the fabrication process. Prior to the step in which an element is turned on, the material stiffness matrix of the element is reduced by the order of  $(10)^6$ , so that its stiffness will be of negligible influence on the structure before the element is turned on.

### 3.9 Program Load Step Operation

When a new load step is initiated several things happen within the computer program. The elements being turned on in the current load step have their element stiffness calculated by using a fiber direction modulus which is reduced by setting it equal to the transverse modulus. It is reduced because the application of the nodal loads in this load step with unreduced properties would generate large fiber direction stresses within the element. These



generated stresses would then combine with the initial stresses of the element such that the final computed stress state of the element would be quite different from its applied initial stress. The stress state of an element when it is just turned on and added to the structure should ideally be equal to its initial value. By using reduced fiber direction material properties and hence reduced elemental stiffness, the fiber stresses generated within the load step due to the nodal forces are small. Thus the element does not support much of the nodal loads created from the initial stresses in that load step, and the initial stress state is preserved. In successive load steps the full element stiffness matrix is used.

The nodal loads for a load step are calculated using the right hand side of equation 3.7-3. The  $[B]^t$  matrix is calculated using full orthotropic material properties of the layer just turned on (rather than the reduced properties used in the structure stiffness matrix). This gives a vector of nodal loads due to the initial stresses of the layer just turned on or added to the structure. This loading procedure applies the necessary step-by-step loading as each layer is applied with the elements being turned on in the required load step.

As the analysis proceeds, if an element of the composite material loses all of its initial tension stress in the

fiber direction and tries to support fiber direction compression the material stiffness matrix of that element is modified because the uncured composite cannot support fiber direction compression. The modification creates an isotropic set of material properties by reducing the fiber direction modulus as in the elements newly turned on but for a different reason. This allows the material that has lost all initial tension to support bulk compression without the high fiber direction stiffness. These elements of lost fiber tension would likely have degraded strength, especially if micro or macro-buckling occurred in that layer due to excessive fiber direction compression.

## Chapter 4

### Analysis Procedure

#### 4.1 Definition of the Problem

The problem to be investigated was the strength loss in filament wound spherical pressure vessels. The source of strength loss studied here is assumed to be related to degraded fibers within the composite. Degraded fibers are ones which undergo compressive hoop strains during the manufacturing process, and end up cured in a localized buckled configuration. In order to identify fibers which are subjected to compressive hoop strains a finite element model was developed that simulates the actual layer-by-layer fabrication process.

Several assumptions were made to ease the modeling of the sphere. The sphere was considered to be symmetric about the equator so that each hemisphere could be considered independently. The sphere was also considered to be symmetric about the polar axis which passes through the center of the fill tube. This assumption of symmetry about the polar axis applies to the geometry, loading and material. It is also assumed that the material in any layer is uniformly distributed around this axis of symmetry.

The analysis is divided into three main sections and one supporting section, each requiring its' own computer

program. The three main sections being 1)Pattern simulation, 2)Mesh generation, and 3)Finite element analysis. The supporting section is data preparation for the finite element program.

#### 4.2 Pattern Simulation

The first step in modeling the filament wound sphere is to simulate the winding pattern. This simulation is carried out by a computer program called NTHICK. The instructions on how to create an input file for NTHICK are given in Appendix C.

Some of the data that must be acquired for input is described below. The outside radius of the spherical form, the thickness of one band and a sequence number must be specified. If the number is 1, the sequence will be such that the band sets are applied progressively from the pole to the equator - commonly called a downwind. If the number is 2, the sets are applied from the equator to the pole - upwind. Normally a sphere will have a downwind followed by an upwind to produce a balanced sphere. Both the downwind and upwind are complete patterns.

The number of polar angular increments must be specified which gives the number of finite elements to be created along the meridian. The lengths of the elements along the meridian may be specified in up to five different regions.

This sequence allows for a finer mesh in areas of likely stress concentrations. The angular coordinates of the band edges along with the number of bands in each set must then be specified. This data is entered in the order of the winding sequence for each band set.

The output from the pattern simulation program NTHICK creates an ordered file, to be used later as an input file for the mesh generating program SPHMESH. The first line of the output specifies the number of band sets and the number of calculating (polar) positions used. Then at each calculating position the polar position (angle between the pole and the calculating position) and the total fiber laminate thickness are generated, followed by data for each layer giving the fiber angle orientation (angle between the fiber and latitude in the tangent plane) at the band segment edges and the thickness contribution of that layer.

#### 4.3 Generating the Mesh

The second step in modeling the filament wound sphere is to generate a mesh over the sphere. The mesh generating program, SPHMESH, uses the output from the thickness calculation and pattern simulation program, NTHICK, together with another input file to control the generation of the elements. The instructions on how to create the other input file for SPHMESH are given in Appendix D.

The input file contains two program options; IGRAPH and IMODE. If IGRAPH is 0 the graphics routine is not run, if 1 the graphics routine is activated and the mesh can be seen on the screen and a hard copy can be made. If IMODE is 0 the output is formatted with headings for checking the data, if 1 the output is formatted for direct input into the data preparation program COUPLE.

The physical size of the fill tube and the spherical form must be specified along with the required element density. The size of the fill tube is specified by the inside diameter, D1, the outside diameter, D2, and the height above the spherical form, H. The spherical form is specified by the inside radius, R, and the thickness of the form, TLAY(1,1). The first polar angle, PANG(1), must be specified as the intersection of the outside diameter of the fill tube and the outside surface of the spherical form. The element density for the fill tube is controlled by specifying the number of elements up and through the fill tube, NV and NH respectively. The element density for the spherical form and the composite is controlled by the number of elements through the spherical form and composite, NF and MR respectively.

The last few data entries control the graphics routine. The first entry in this sequence controls the plot, ITETT, if 0 a full plot of the mesh is drawn, if 1 a partial plot

is drawn in which the following additional two entries are required, ISTART and IFIN. Where ISTART is the starting node number for the plot and IFIN is the finishing node number, giving the node number range to be included in the plot.

#### 4.4 Generating the Input to COMSPH

All the necessary data to run the finite element program, COMSPH, is put together in a program called COUPLE. This program takes the output from the mesh generating program, SPHMESH, and combines it with another input file to produce the required format for COMSPH. The input instructions for creating the input file for COUPLE are given in Appendix E. The other data that COUPLE requires to create the input file for COMSPH is: HED, the title to be printed on the output; NUMEG, the number of element groups; NLCASE, the number of load cases which usually is equal to the number of fiber layers; MODEX, a solution mode option - if 0 data check only - if 1 full execution of the program; NVECT, a nodal load print control option - if 0 does not print nodal load vector for each load case - if 1 it prints the nodal load vector for each load case; NOUT, output suppression option - if 0 does not suppress the output - if 1 all but the last load step output is suppressed.

The next group of data controls the loading sequence for externally applied nodal loads. If there are no externally

applied loads within a load step and the program is to generate nodal loads from the initial winding tension, a load case number, LL, must be assigned together with zero applied nodal loads, NLOAD. If external nodal loads are applied in a load step, for each load the node number to which it is applied, NOD, the direction of the load, IDIRN, and the magnitude of the load, FLOAD, must be specified. The element control data are element type, NPAR(1), and the number of different material properties sets, NPAR(3). For axisymmetric elements NPAR(1)=3. In this case there are two sets of material properties, one set for the spherical form and one set for the composite, NPAR(3)=2. For each material property set there are eight inputs, the material property set number, N, three Young's moduli for orthotropic materials, E(1,N), E(2,N), E(3,N), three Poisson's ratios, NU-23, NU-31, NU-21, and the shear modulus, G-12. If the material is isotropic only three entries are needed in their correct places; material property set number, the first Young's modulus and the first Poisson's ratio.

The last input into COUPLE is the initial winding tension in each fiber layer, TENS(I).

#### 4.5 Running COMSPH

The output file from COUPLE contains all the input necessary to run the finite element analysis program COMSPH. If the data to run COMSPH is to be assembled by hand, the



input instructions are given in Appendix F. A complete listing of the program COMSPH is not included as it is quite long, but a detailed description of how the program operates is given in Appendix G. The output from COMSPH is suppressed by the option NOUT, if 0 it prints all the output, if 1 it suppresses most of the output. When the output is suppressed the output file contains the input data and the program generated data (nodal points and elements). Also the elemental stresses and accumulated stresses are printed for the last load step in both the global and fiber coordinates. The average stress and strain in fiber directions for each layer are also printed when the output is suppressed. When NOUT=0 the output will include the nodal displacements for each load step, the elemental stresses for each load step and the accumulated stresses after each load step.

#### 4.6 Creating a Strength Map

Once the average strain in each layer is found a strength map can be created using the results from reference 1. A strength is assigned to each layer depending on its residual strain. If the residual strains for a layer are positive, i.e., the layer is still in tension, full fiber strength is assigned. If the residual strain is negative, i.e., the layer has gone into compression with perhaps some buckling occurring, a strength is assigned from the graph of residual

strain versus strength from reference 1.

## Chapter 5

### Results

A portion of the spherical vessel to be modeled was the first two shells of the vessel presented in reference 13. A shell is a complete set of bands that provide uniform thickness over the spherical form. The vessel has six shells in total with each shell containing twelve layers. The vessel composite is allowed to cure after the application of the first two shells. The model contains only the first two shells as the objective of this analysis is to predict potential strength loss due to tension loss and microbuckling of fibers on a low stiffness mandrel. Once the two shells are cured the winding form becomes considerably stiffer and further tension losses are negligible.

The vessel is a 4.000 in. (101.6 mm) inside diameter sphere with a copper form 0.040 in. (1.02 mm) thick. There is one stainless steel fill tube, 0.062 in. (1.57 mm) inside diameter and 0.188 in. (4.78 mm) outside diameter. The model of the fill tube varied from the actual fill tube by assuming the fill tube to be made of copper and to have a height of 0.280 in. (7.11 mm), just enough to protrude through the two shells. The winding pattern used was the delta-axisymmetric pattern using a composite of Kevlar 49/epoxy. The average thickness of the two shells is 0.239

in. (6.07 mm) compared to an average thickness of 0.718 in. (18.24 mm) for the full composite. The thickness of the composite is calculated at 36 polar positions by the thickness calculation and pattern simulation program, NTHICK.

### 5.1 Pattern Simulation

The pattern is described in Appendix A. The nominal band width for the pattern design is 7.5 degrees of arc coverage, and the band thickness is 0.0053 in. (0.135 mm). The first polar position angle is 2.647 degrees. The pattern has two shells of winding, a downwind followed by an upwind. There are twelve band sets to each shell and each band set is treated as a layer in the process model.

The pattern is fed into the thickness calculation and pattern simulation program to calculate the fiber orientation angles and the layer thicknesses at specified polar positions. The following input data together with the pattern description produces the thickness profile : radius, 2.040 in. (92.62 mm); thickness factor, 0.0053 in. (0.135 mm); number of band sets, 24; number of polar increments, 36. The first twelve bands are in a downwind sequence, the second twelve are in an upwind sequence. The material stacking sequence is specified as 1 for the downwind and 2 for the upwind. The size of the polar (meridian) angle increment is 1.353 degrees for the first one then 1.5

degrees out to the 34 degree polar position and 4 degrees for the remainder.

The output from NTHICK lists the number of fiber layers, 24 and the number of polar positions for the simulation, 36. Then for every polar position the polar angle and total fiber composite thickness are output. This is followed by the layer thickness, the starting, and the finishing fiber angles for every layer of the composite. Part of the output is given in Appendix B. This is the thickness profile for the first and last polar positions. The first two and the last two layers are present at the first polar position, all the other layers are indicated by zeros. All 24 layers are present at the last polar position. The output is fed into the mesh generating program, SPHMESH, to generate the finite element mesh.

## 5.2 Mesh Generator

The thickness profile and fiber angles are fed into the mesh generator along with other data to produce the nodal point and element data which describe the finite element mesh. The other data necessary to create the mesh are two options IGRAPH and IMODE: with IGRAPH=1 the mesh is drawn on the screen ; with IMODE=1 the output file for COMSPH is created. The remaining data controls the actual mesh generation. The data used in the model follows: inside diameter of the fill tube, 0.062 in. (1.57 mm); outside

diameter of the fill tube, 0.188 in. (4.78 mm); height of the fill tube, 0.280 in. (7.11 mm); inside diameter of the spherical form, 2.000 in. (50.8 mm); first polar position angle, 2.647 degrees; thickness of the spherical form, 0.040 in. (1.02 mm); number of elements up the fill tube, 24; number of elements across the fill tube, 4; number of elements through the spherical form thickness, 4; and the number of elements through the fibers, 24. The final three pieces of data control the graphical output. The first of these three is a plot control, ITETT; ITETT=0 for a full plot, and ITETT=1 for a partial plot. If a partial plot is required ISTART and IFIN are specified as the starting and finishing node numbers for the plot. The fill tube region, for example, uses ISTART=1 and IFIN=314.

### 5.3 Mesh Generator Output

The output from the mesh generator is in two forms, 1)a data file that contains all the nodal point and element information (IMODE=1), and 2)a graphic visualization of the created mesh (IGRAPH=1).

The mesh starts at the inner edge of the fill tube with the first four columns representing the fill tube. The mesh continues along the meridian in columns of four elements to the equator. This group of elements model the fill tube and the spherical form that the fibers are wound around. They are assigned elastic properties of the form's material. The

elements describing the layers of fibers start at the outer edge of the fill tube on the surface of the form. The element numbering sequence is in radial columns along the meridian to the equator for each layer. The number of nodal points along each radial line for each layer is dependent upon the fraction of the layers thickness to total fiber thickness. The total number of nodal points at any polar position for the fibers is 24. Each element is assigned orthotropic elastic properties in fiber coordinates which are transformed to model coordinates within the finite element program.

The element length along the meridian varies to allow for a finer mesh in the fill tube region. The elements nearest the fill tube have lengths corresponding to 1.5 degree increments along the meridian, except for the first element which has a length of 1.353 degrees. This relationship applies out to the twenty second polar position. The next group of elements have lengths of 4 degree increments out to the equator.

The finite element mesh generated for the 24 layer model is shown in Fig. 19. The mesh shows the relatively uniform total thickness that the two shells of composite form. It is very difficult to distinguish the boundaries of the 24 fiber layers from the mesh plot. An attempt to highlight the layers with heavy lines has been added by hand. Three

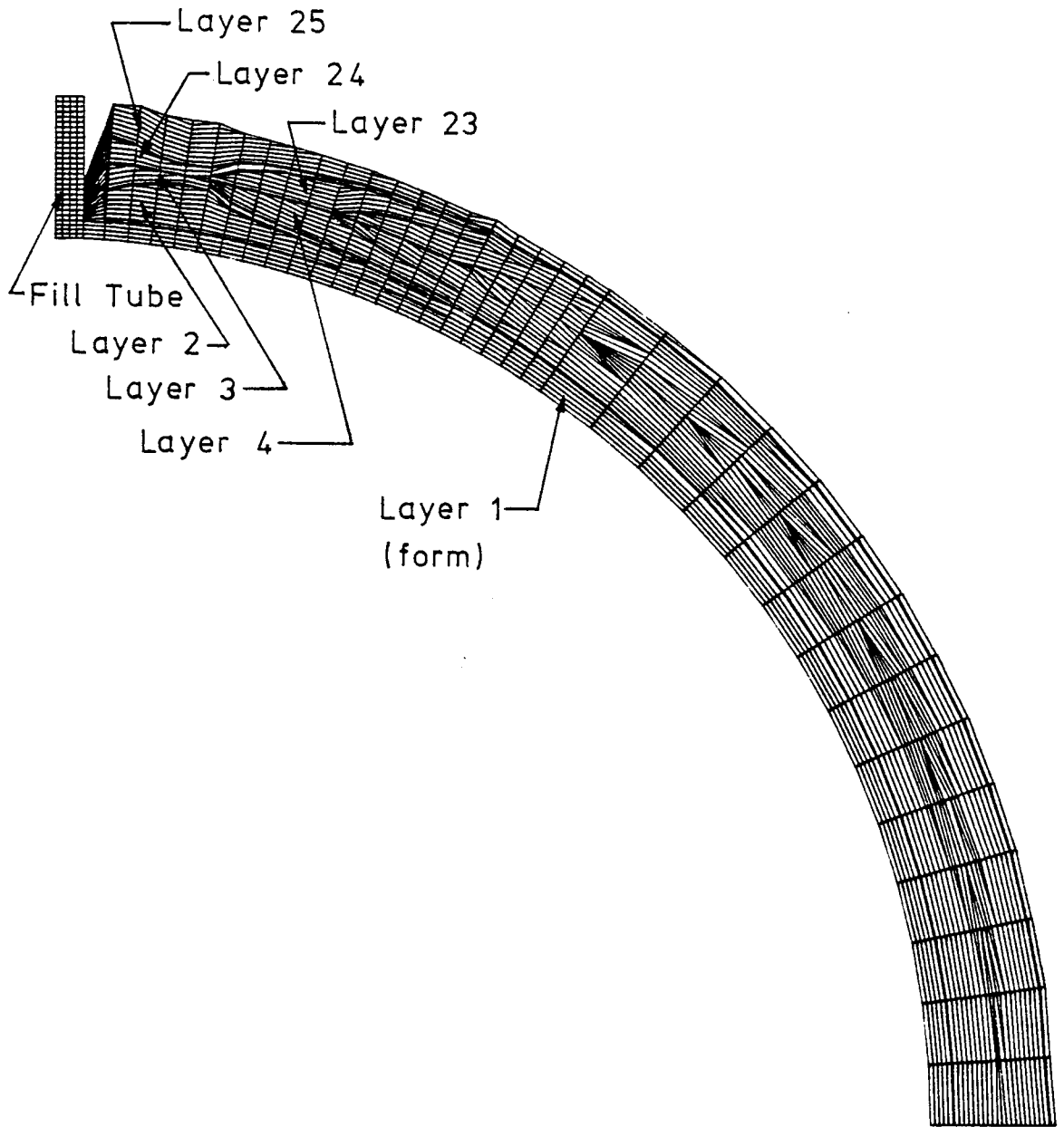


Figure 19. Full Generated Mesh for the Process Model.



regions of the mesh are expanded to show more clearly the mesh in these areas of interest. The regions expanded are the fill tube, the transition from 1.5 degree element lengths, to 4 degree element lengths and the equator region.

The expanded region of the fill tube is shown in Fig. 20. The four layers present can be clearly seen in the first four columns of elements, they are the first two and the last two fiber layers. They correspond to model layer numbers of 2, 3, 24, and 25 as the copper form is considered to be the initial layer (layer 1) but with different material properties. Layers 4 and 23 start in the fifth column of elements. There are two things to notice in this portion of the mesh, 1)there is no constraint between the fill tube and the fibers, and 2)the thickness of the composite at the fill tube is thinner than the rest of the composite.

The transitional area of element lengths is shown in Fig. 21. There are three columns of elements with lengths of 1.5 degrees and three columns of elements with lengths of 4 degrees. The first column of elements includes fiber layers 2 through 6, and 21 through 25. Layers 7 and 20 start at the element length transitional point with layers 8 and 19 starting in the last column of elements in this region.

The expanded equatorial area is shown in Fig. 22. The first column in this area includes fiber layers 2 through

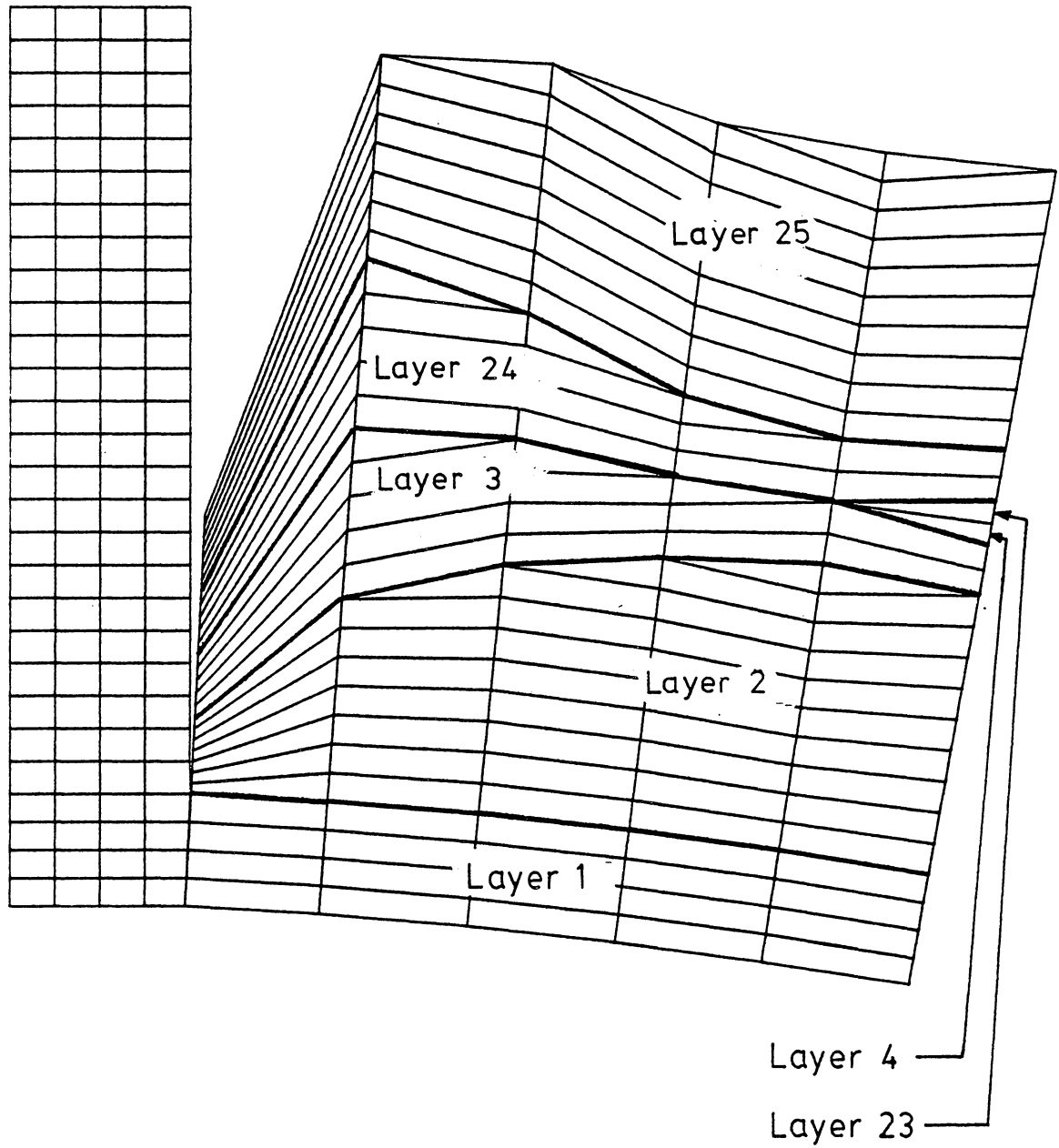


Figure 20. Expanded View of the Mesh around the Fill Tube.

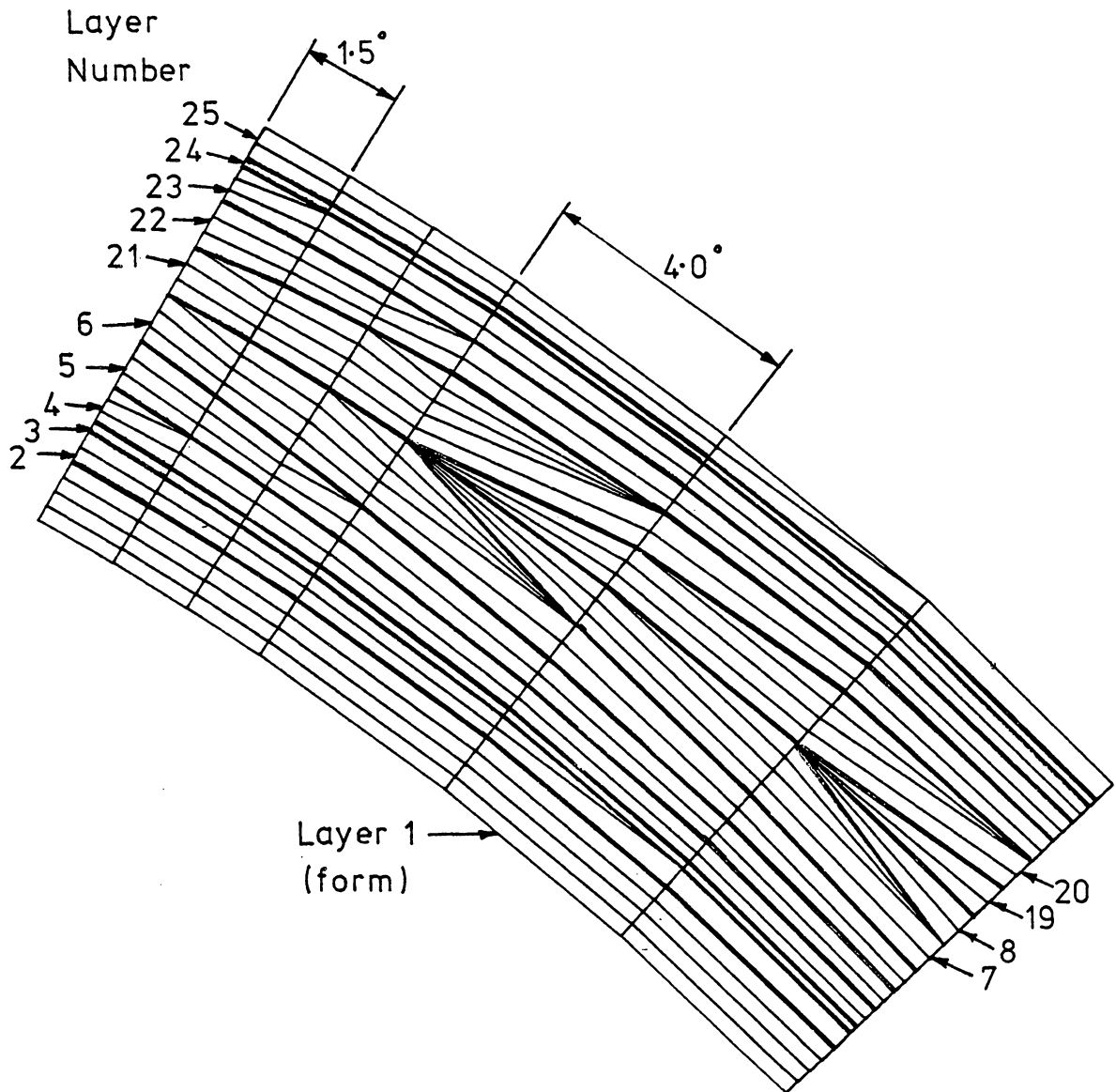


Figure 21. Expanded View of the Mesh at the change of Element Length.

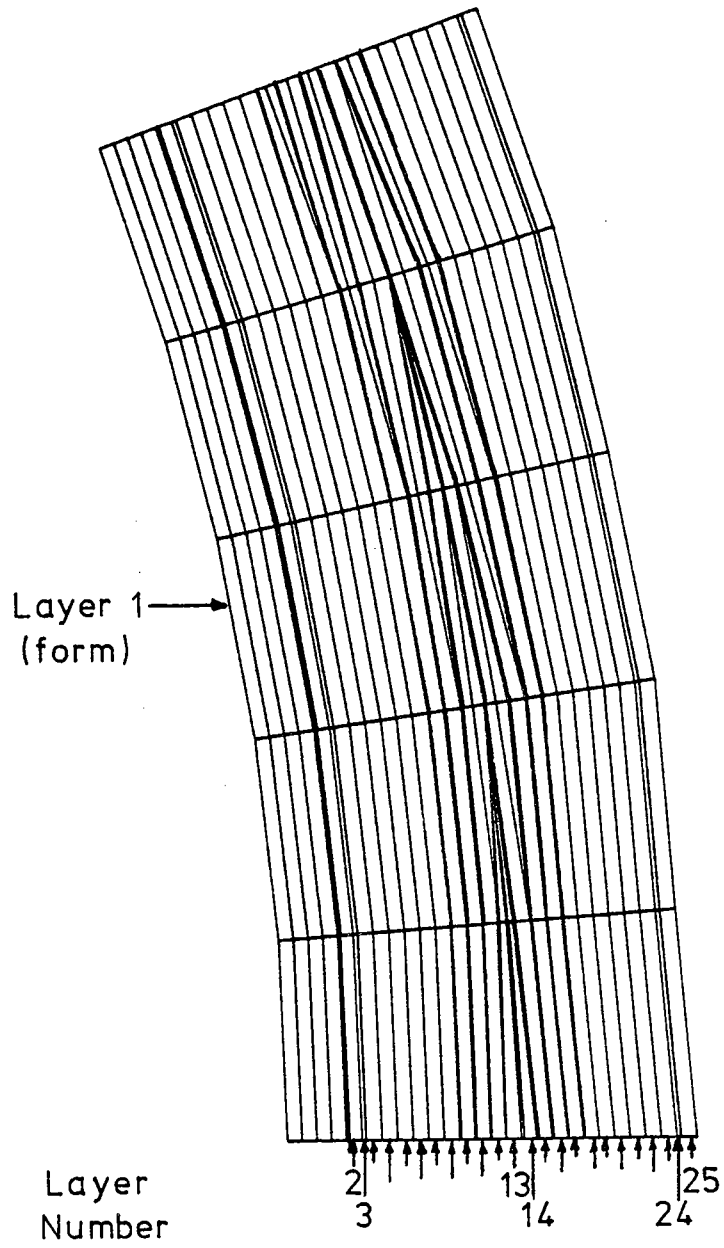


Figure 22. Expanded View of the Mesh at the Equator.

11, and 16 through 25. Layers 12 and 15 start in the second column of elements with layers 13 and 14 starting in the fifth column. In the last column of elements there is only one element per fiber layer.

An estimate of the total number of fiber elements is 35 times 24 which equals 840 elements, and the number of elements in the fill tube and form is 252. This gives a total number of 1092 elements for the model, but the mesh generator generates 1170 elements for the same model. The mesh generator takes into account the profile of the fiber layers and assigns triangular elements to accommodate large changes in the profile from one polar position to the next. The number of nodes are fixed along each polar line. Because triangular elements are used for transitions the number of elements created increases.

The output from the mesh generating program contains all the node and element information necessary for the finite element program. The finite element program also needs some other data to run correctly. This other data controls the various options and loading patterns built into the program. The output from the mesh generating program is combined with this other data in a program called COUPLE. This program arranges all the data necessary to run the finite element program COMSPH into the correct order.

#### 5.4 COUPLE Output

The output from COUPLE is the complete set of data that is necessary to run the finite element program COMSPH. The data file contains all the control and option information as well as all the nodal point, element, and material property data for the model's analysis. The data file is created such that it is in the correct order as defined by the input to COMSPH.

The output from SPHMESH is fed into COUPLE together with the data file given in Appendix A to create the input file for COMSPH. The output files from SPHMESH and COUPLE are not given because they are very large. After the output data file is prepared for COMSPH the finite element program is run.

#### 5.5 Finite Element Output

The model was created using an initial fiber direction tensile stress of 15.836 kpsi (109.2 MPa) in each layer. This corresponds to a residual (initial) winding force of 500 grams (4.91 N). The correlation of spool tension to residual tension used in reference 1 indicates that a spool tension of 681 grams (6.68 N) would be necessary to manufacture the sphere. The spool tension is the tension that is applied to the fibers as they are wound onto the sphere from a spool. The residual tension is the tension

left in the fibers after a layer has been wound onto the sphere. The difference between them is an allowance for resin flow based on the results from reference 1.

The output from the finite element program, COMSPH, is extremely large, therefore most of the output is suppressed using the NOUT option. The output using the suppression option is still quite large, about 9000 lines. The suppressed output contains all the nodal point, element, material, and external load data that was input to the program. The element stresses for the last load step together with the accumulated element stresses are output in both global (model) and fiber coordinates. The last section of the output is the final condition of the model. The average residual layer stresses (fiber direction) have been computed by averaging the fiber direction stress component independently and by averaging fiber strains and then computing the average stress. The average residual layer strains have been computed, this gives an indication of the layer's strength.

The average fiber stresses and strains for each layer in this test case are given in Table 1. The first layer or mandrel has an average  $t$  direction compressive stress of 21.795 kpsi (150.3 MPa) which is above the material yield strength of 10 kpsi (68.95 MPa). The average layer stress in Table 1 shows a difference for the first three (2, 3, and

Table 1 Average Layer Fiber Direction Stress and Strain

Layer Number	Average Stress		Average Strain in/in (mm/mm)
	By Stress kpsi	By Strain kpsi	
1	-0.22535E+05	-0.22535E+05	-0.93114E-03
2	0.83622E+04	0.38227E+04	0.37488E-03
3	0.10542E+05	0.60852E+04	0.55928E-03
4	0.94303E+04	0.60285E+04	0.55681E-03
5	0.65888E+04	0.65888E+04	0.59742E-03
6	0.63529E+04	0.63529E+04	0.57181E-03
7	0.62415E+04	0.62415E+04	0.55940E-03
8	0.61048E+04	0.61048E+04	0.54855E-03
9	0.62800E+04	0.62800E+04	0.56528E-03
10	0.70812E+04	0.70812E+04	0.63410E-03
11	0.84051E+04	0.84051E+04	0.74428E-03
12	0.97730E+04	0.97730E+04	0.85574E-03
13	0.10179E+05	0.10179E+05	0.88821E-03
14	0.10736E+05	0.10736E+05	0.93264E-03
15	0.12251E+05	0.12251E+05	0.10559E-02
16	0.13315E+05	0.13315E+05	0.11428E-02
17	0.13654E+05	0.13654E+05	0.11686E-02
18	0.13547E+05	0.13547E+05	0.11562E-02
19	0.13191E+05	0.13191E+05	0.11222E-02
20	0.12801E+05	0.12801E+05	0.10854E-02
21	0.12666E+05	0.12666E+05	0.10691E-02
22	0.12862E+05	0.12862E+05	0.10823E-02
23	0.13720E+05	0.13720E+05	0.11495E-02
24	0.13832E+05	0.13832E+05	0.11590E-02
25	0.15836E+05	0.15836E+05	0.13197E-02

To convert from kpsi to MPa multiply by 6.895.



4) fiber layers between averaging by stress and averaging by strain. The difference being that in the averaging by stress if any element has resultant compressive fiber direction strains its stresses are calculated with reduced material properties because the uncured composite cannot support compressive stress. These reduced compressive stresses when averaged with the remainder of the layer cause the average stress to be higher than if the high compressive stresses were included. The averaging by strain includes both tensile and compressive values and results in a lower average stress when compressive strains are present in some elements of a layer.

The elements that have resultant compressive strain in the first three fiber layers (2, 3, and 4) are indicated in Fig. 23 by the shaded elements. These compressive strain elements are on the inner surface of the first fiber layer, 2, starting at the seventh polar position line. The compressive strain elements are not through the whole layer thickness until the eighteenth polar position line and then they continue to the equator. The compressive strain elements for the second fiber layer, 3, also start at the seventh polar position line. The compressive elements go through the whole thickness at this position and around to the equator. The compressive strain elements for the third fiber layer, 4, follow the same general pattern, but no continuous block of compressive elements appear. They are

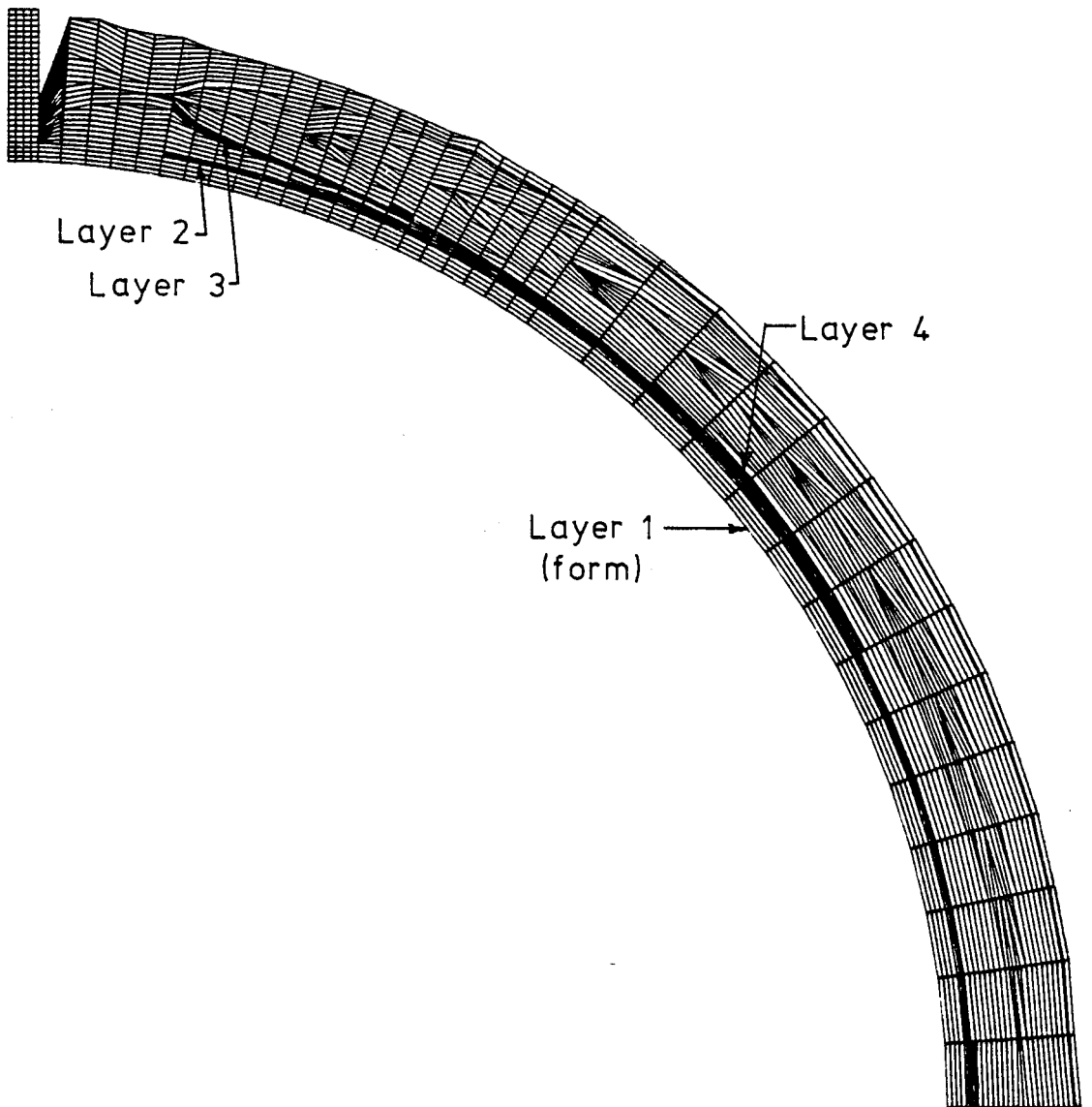


Figure 23. Elements with Resultant Fiber Direction  
Compressive Strain.

intermixed with resultant tensile strain elements.

These elements with resultant compressive strain that appear in the first three fiber layers are not enough to result in total tension loss in any of these layers. Since strength loss is based on average layer tension loss no strength reduction is applied in this case. There may be some strength loss as indicated by some elements with resultant compressive strains, but the amount of strength loss is difficult to predict.

The general pattern of layer tension loss looks rational. The inner layers have more tension loss than the outer layers. The slight differences in tension loss are due to the different fiber directions in the layers, as well as the varying layer thicknesses.

## Chapter 6

### Discussion

#### 6.1 Mesh Generator

The function of a mesh generating program is to create the finite element mesh by specifying all the nodal point and element data. This often saves the operator the time and effort of specifying them by hand. Also, the chance of human error is reduced. Mesh generating programs can be very general or very specialized as in this case. This mesh generating program is specifically designed to handle spherical vessels. The program is further restricted in that there must be a fill tube and there must be at least one fiber layer beyond the form (mandrel). The program ensures that for every layer of the composite there is at least one element throughout the thickness. The minimum of one element per layer is ensured by placing a nodal point at every interlayer boundary. The number of nodes throughout the thickness is constant. This keeps the bandwidth of the assembled stiffness matrix as small as possible. The program generates only quadrilateral elements, but these can be modified by forcing two adjacent corners of the quadrilateral together to form a triangular element.

The mesh of quadrilateral and triangular elements produced by the mesh generator as shown in Fig. 19 is about twice actual size. The profile of the mesh appears to form

a constant thickness from the fill tube to the equator. The thickness of an individual layer varies from the fill tube to the equator. The graphics routine of the program draws the mesh layer-by-layer, but it does not make any distinction between them on the hard copy. It is very difficult to trace the outline of a single layer by hand in Fig. 19 as the elements of the mesh are very small. Figures 20, 21, and 22 show sections of the same mesh enlarged by the graphics routine. The amount of enlargement is scaled by the graphics routine. The enlargement fits into a square, 6 in. by 6 in. The enlargement can be changed by specifying the square to any size, up to the machine's capacity. The section to be enlarged is determined by two nodal point numbers, the start and end point nodal numbers of a range. The elements within these enlarged sections are larger and the outline of layers can be more easily traced as shown by the heavy lines which were darkened by hand.

The section of the fill tube and the first five columns of elements as shown in Fig. 20 have four fiber layers next to the fill tube and six fiber layers at the end of this section. The layers are numbered in the fabrication lay-up sequence. That is the layers start from the spherical form (the spherical form is called layer number 1) with layers 2, 3, 24, and 25 in the column next to the fill tube, and layers 2, 3, 4, 23, 24, and 25 are in the fifth column of elements. The fifth column of elements gives birth to

layers 4 and 23. The layers will always be born in pairs in a symmetrical fabrication with one in the downwind sequence and one in the upwind sequence as both sequences are complete winding patterns. The number of layers present within any section increases as the equator is approached where all 24 layers are present.

Figure 21 shows the enlarged section of mesh where the element length changes from 1.5 degrees of arc to 4 degrees of arc. The first column of elements (left-hand side) in this section represent layers 2 through 6, and 21 through 25. Layers 7 and 20 start in the first 4 degree column of elements and layers 8 and 19 start in the last column of elements of this section.

The last five columns of elements leading down to the equator are enlarged in Fig. 22. The first column of elements in this final section contains all layers except layers 12, 13, 14, and 15. Layers 12 and 15 start in the second column of elements, and the last two layers, 13 and 14, start in the next to last column of elements. Thus only the last two columns of elements contain all 24 fiber layers.

In these last few columns the pattern of quadrilateral and triangular elements that make up the mesh are not symmetric in the upwind and the downwind. The layer thicknesses of corresponding layers in the upwind and

downwind are the same and therefore they should have the same element formulation. The difference between the upwind and downwind is caused by the formulation of elements. The formulation starts at the inner surface of the downwind and proceeds through the layers to the outer surface of the composite. The nodal point positioning scheme uses an accumulative error check throughout the layer build up to ensure that the total number of nodal points along a polar position line is constant. This means that while the number of nodal points in the upwind and downwind are the same their position with respect to their joint boundary are different.

If the pattern of elements needs to be the same in both the upwind and downwind the nodal point positioning scheme would need to be modified. One possible way would be to make the scheme position nodal points across a winding pattern (upwind or downwind) in the same direction as their symmetry. In this case nodal points would have to be placed in the upwind through layers 2 to 13 and in the downwind through layers 25 to 14. This could become difficult to incorporate for general use.

## 6.2 Element

The reasons for choosing the isoparametric quadrilateral element are many. They fall within two groups; 1) physical considerations and 2) theoretical considerations.

There are basically three physical considerations; 1) does the element model the boundaries of the form reasonably, 2) does the element lend itself to automatic mesh generation, and 3) the physical aspects of data preparations for the element.

Making a model to approximate the boundaries of a circular ring can be done with virtually any element shape. The difference being the number of elements needed to acquire a good approximation. The isoparametric quadrilateral element usually will require less elements than triangular elements but probably more than elements with curved edges. The automatic mesh generation for virtually all other two-dimensional elements are more complex in the placement of nodal points and in the formation of element connectivity. Higher order elements (more degrees of freedom per node and more nodes per element) usually require more data preparation routines than the simple elements.

As the layers within the composite change thickness some means of allowing for this must be made. The simplest solution would be to keep the number of elements within a layer constant and just change their thicknesses. This is not practical as some layers are not present at all positions, and elements with zero thickness will cause the stiffness matrix to become singular. A better solution



would be to change the number of elements as necessary along the layer to accommodate the changes in layer thickness. This would give a layer with step changes in its boundary, and, therefore, is not a very good approximation. The solution chosen was to allow some of the quadrilateral elements to collapse to form triangular elements. These triangular elements allow a smoother approximation of the layer boundary.

The triangular elements are formed by allowing two corner nodes of the quadrilateral element to occupy the same space. This makes the triangular element sensitive to the node numbering order of the element. This is called anisotropy. For example, if a triangular element was formed by connecting nodes 18, 25, and 19 (19 being the collapsed corners of the quadrilateral element) an elemental stiffness could be calculated. Now change the node order to say 25, 19, and 18, a different elemental stiffness would be calculated. The element stiffness changes because one of the nodes of the triangle represents two nodes of the quadrilateral. Since all the elemental stiffness calculations use the nodal point coordinates, one corner node of the triangular element is used twice as the formulation is quadrilateral. This sensitivity to node order gives a poorly conditioned element. Some of the anisotropy was removed by reducing the order of the numerical integration from the four point quadrature scheme

to a single point quadrature.

The anisotropy could be removed completely by formulating a separate triangular element. This would involve the addition of three more subroutines to the finite element program and make the assignment of storage with the dynamic A array more difficult. Since the number of triangular elements necessary in modeling the sphere is very small the error produced by the anisotropy of those elements would also be small. Therefore, the effort necessary in creating correct triangular elements was estimated to be excessive for the anticipated improvement.

The use of higher order elements usually gives better results and requires fewer elements than with the use of simple elements. The disadvantage of higher order elements is that the formulation of the element is more complex and time consuming. Higher order elements usually require higher orders of numerical integration. Also the coupling of different types of higher order elements together to approximate boundaries is much more difficult than with simple elements.

### 6.3 Finite Element Program

The finite element program, COMSPH, is a specialized program for the analysis of filament wound spheres. The major difference between this program and a general finite

element program is the IOFFON option. The purpose of the IOFFON option is to reduce out elements that are not required at the current load step. Another difference in this program is that elements which have compressive fiber direction stress use reduced material properties.

Elements which are not required in the current load step have their elemental stiffness reduced by a factor of  $(10)^6$ . If the element is not required its stiffness should have as little effect on the current structural stiffness matrix as possible. The reduction factor of  $(10)^6$  was chosen as this is of the same order of magnitude as the elemental stiffness. When the reduced element's stiffness is added to the structural stiffness matrix little change should occur in the matrix. If the factor is too large the stiffness matrix may become ill-conditioned, and if the factor is too small the added elemental stiffness would significantly change the stiffness matrix.

This program reduces the material properties of elements which have compressive fiber direction stresses. The reduction is to change the fiber direction Young's modulus to equal the transverse direction value. The reduction is necessary since wet fibers cannot withstand forces in compression as they can in tension. The reduction to transverse values is probably a good assumption since the fibers are in the wet state, i.e., surrounded by epoxy

resin. A single unrestrained fiber would buckle under a very small load, but a band of fibers completely surrounded by other bands is constrained. As the compressive force increases some localized buckling will occur. The constraining force is a function of the transverse Young's modulus of the surrounding fibers. Since the resin will transmit any force hydrostatically, the compressive force is assumed to also be a function of the transverse Young's modulus of the surrounding fibers. Exactly how much of a function depends on how the fibers are spaced, the tightness of the wind, and the ratio of the fibers to resin.

The finite element program calculates the average layer stress and strain in fiber directions. This gives an indication of any strength reduction due to localized buckling of the fibers. The average stress was calculated by two means; 1) by averaging the fiber direction stress of the elements within a layer, and 2) by averaging the elemental strains within a layer.

The two methods yield different values for average stress in the test case for the first three fiber layers and match for the remaining layers. The difference is in the use of reduced material properties for the elements experiencing resultant compressive strains. The strain that an element experiences is the same whether its material properties have been reduced or not. When an element has reduced properties

the amount of stress increment added to the accumulative stress is also reduced. As the load step stresses are added to the accumulative stress the reduction is not as large as the addition of load step strain to the accumulative strain. Elements start to receive resultant compressive loading when there is a difference in the two methods of calculating the average layer stress. Degradation of a layer is not assumed to occur until the average strain of a layer goes negative. This means that more elements are under resultant compressive loading than those still in tension and large amounts of buckling within the fibers have occurred.

#### 6.4 Results

In the test case no layers are assigned reduced strengths as the average layer strain is positive for all layers. The first three fiber layers (2, 3, and 4) have some elements with compressive fiber direction strain, but the average strain of these elements is less than the average strain of elements with tensile fiber direction strain. This does not mean that there is some localized buckling of the fibers within these first three layers. Buckling of the fibers is assumed to occur when the average layer strain is negative. The variation of strain around a band path should be small. The finite element analysis shows strain variation from element to element around the band path, therefore, the average layer strain must be used to determine when buckling

occurs. Strength degradation is not applied until the average layer strain is negative. The first fiber layer has the most negative strain elements with the second fiber layer having more than the third fiber layer. This pattern of negative strain elements appears to be reasonable for the winding/loading pattern modeled.

The general pattern of layer tension loss for the 24 layers also appears to be rational. The inner layers generally experience more tension loss than the outer layers. There is no continuous increase in tension loss from the outer fiber layer to the inner fiber layer. This slight variation can be seen in the average layer strain as shown in Table 1. This is possibly explained by the winding pattern and layer loading. Fiber layers 2, 3, 24, and 25 are the only layers that cover the entire spherical form. All the other layers cover varying portions of the spherical form. Layers 13 and 14, for example, cover only a small section near the equator. As these layers are applied the elements directly under them and perhaps a few of the adjacent elements will experience compressive fiber direction strains, while all the other elements in the previous layers may experience tensile fiber direction strains. Some elements will experience both tensile and compressive strain increments during the addition of layers. This makes the exact layer-by-layer tension loss pattern difficult to visualize, but the overall tension loss pattern

still should be more on the inner layers and less on the outer layers as Table 1 indicates.

## Chapter 7

### Conclusions - Recommendations

#### Conclusions

An analytical procedure for modeling the manufacturing process of filament winding for spherical pressure vessels was developed to find the fabricated strain state of the wound layers. This fabricated strain state can then be used to predict the amount of strength degradation in the layers.

Finite element analysis is well suited for the analysis of filament wound structures like spheres. The many different coordinate systems needed to describe the fiber pattern and material properties are easily handled in this analysis procedure.

The equation solver for the finite element procedure was a standard node sequence solver. The bandwidth was minimized by keeping the number of nodal points through the composite constant.

The sphere test case modeled had no degraded strengths as the resultant fabricated strain state for all layers was positive. The model predicts some local degradation as indicated by the difference in resultant fiber direction stress averaged by stress and by strain. Significant degradation is assumed not to occur until the average strain along the band path is negative.



## Recommendations

The average mandrel stress obtained in its present form has no significant value. If the fiber direction angle (BETA) for all the mandrel elements are set to 90 degrees instead of 0 degrees, the average mandrel stress calculated would now be the average polar circumferential stress.

Replacing the collapsed quadrilateral elements used to simulate triangular elements by fully formulated triangular elements would eliminate the error produced by anisotropy of the collapsed elements.

In order to set up an experimental program, model some spheres with and without degradation of layers. Spheres with degraded layers can easily be produced by first winding with low fiber tension and then with high fiber tension on the subsequent layers. Strengths can then be assigned to the spheres based on the amount of degradation. Some test spheres could then be manufactured using the chosen winding patterns and tensions. The spheres would be pressure tested to produce some experimental data for correlation with the predicted strengths.

A further refinement of the process model would be to reduce the bond between the mandrel and the composite. The model currently assumes a no slip bond between the mandrel

and the composite. The composite is in the wet state and some slip between the mandrel and the composite could occur during manufacture.

Further consideration should be given to the loading of the process model. The current loading is to assume that all the fibers within a layer are subject to a constant initial tension stress. In some areas a layer may be many fibers thick and the stress state would no longer be tension in the fiber direction only. Computing the nodal loads using initial fiber direction tension may not be the best method in this situation. It may be beneficial to compute the nodal loads using initial strains rather than initial stresses.

If the winding tension is high and many layers are applied to a thin spherical form, it may be possible for the spherical form to experience plastic deformation. The model currently assumes only elastic deformation and no account is made of the elastic limit of the form's material. The model could be improved by allowing for plastic deformation when the elastic limit of the form's material is exceeded.

## References

- (1) Dobie, M.J., Leavesley, P.J., and Knight, C.E., "Residual Strain and Strength Loss in Filament Wound Rings", Union Carbide Research Contract Y01 Report, August, 1982
- (2) Weibull, W., "Statistical Distribution Function of Wide Applicability", J.Appl.Mech., Vol. 18, No. 3, pp. 293-297, 1951
- (3) Bathe, K.J. and Wilson, E.L., Numerical Methods in Finite Element Analysis, Prentice Hall Inc., 1976
- (4) Ferguson, G.H. and Clark, R.D., "A Variable Thickness, Curved Beam and Shell Stiffening Element with Shear Deformations", Int.J.Numer.Methods.Eng., Vol. 14, pp. 581-592, 1979
- (5) Grigorenko, Ya.M. and Kokoshin, S.S., "Design of Shell Structures by the Finite Element Method", Sov.Appl.Mech., Vol. 15, No. 7, pp. 3-10, July, 1979
- (6) Ashwell, D.G. and Sabir, A.B., "A New Cylindrical Shell Finite Element Based on Simple Independent Strain Functions", Int.J.Mech.Sci., Vol. 14, pp. 171-183, 1972
- (7) Feijoo, R.A., Jospin, R.J., Bevilacqua, L., and Taroco, E., "A Curvilinear Finite Element for Shells of Revolution", Int.J.Numer.Methods.Eng., Vol. 16, pp. 19-33, 1980
- (8) Kanok-Nukulchai, W., "A Simple and Efficient Finite Element for General Shell Analysis", Int.J.Numer.Methods.Eng., Vol. 14, pp. 179-200, 1979
- (9) Cook, R.D., Concepts and Applications of Finite Element Analysis, John Wiley and Sons, Inc., 1981
- (10) Zienkiewicz, O.C., The Finite Element Method, McGraw Hill Book Company (UK) limited, 1977
- (11) Chen, M.C., and Clewlow, L.N.O., "Computer Analysis of Filament - Reinforced Metallic - Spherical Pressure Vessels", Computers and Structures, Vol. 7, pp. 93-102, 1977

- (12) Knight, C.E., "Analysis of Stresses in Filament - Wound Spherical Pressure Vessels Produced by the Delta - Axisymmetric Pattern", Oak Ridge Y-12 Plant, Report Number: Y-1972, August, 1975
- (13) Knight C.E., "Analytical Failure Prediction of Spherical Composite Pressure Vessels", Journal of Pressure Vessel Technology, Vol. 104, pp.229-231, August, 1982
- (14) Clough, R.W., and Woodward, R.J., III, "Analysis of Embankment Stresses and Deformations", J.Soil.Mech.Found.Div., Proc.Am.Soc.Civ.Eng., July, 1967
- (15) Duncan, J.M. and Clough, G.W., "Finite Element Analysis of Port Allen Lock", J.Soil.Mech.Found.Div., Proc.Am.Soc.Civ.Eng., August, 1971
- (16) Portnov, G.G., and Spridzans, Yu.B., "Winding Glass-Reinforced Plastic Rings Under Programmed Tension", Polym.Mech., No. 2, pp. 361-364, March-April, 1971
- (17) Cain, W.D., and Knight, C.E., "Application of Weibull Criterion to Failure Prediction in Composites", Union Carbide-Nuclear Division, Technical Report Y2235, April, 1981
- (18) Knight, C.E., Jr., "Failure Analysis of the Split-D Test Method ASTM Special Technical Publication", STP-617, March, 1976
- (19) Imafuku, I., Koderu, Y., Sayawaki, M., and Kono, M., "A Generalized Automatic Mesh-Generation Scheme for Finite Element Method", Int.J.Numer.Methods.Eng., Vol. 15, pp. 713-731, 1980
- (20) Frederick, C.O., Wong, Y.C., and Edge, F.W., "Two-Dimensional Automatic Mesh Generation for Structural Analysis", Int.J.Numer.Methods.Eng., Vol. 2, pp. 133-144, 1970
- (21) Pissanetzky, S., "Kubik: An Automatic Three-Dimensional Finite Element Mesh Generator", Int.J.Numer.Methods.Eng., Vol. 17, pp. 255-269, 1981
- (22) Zienkiewicz, O.C., and Phillips, D.V., "An Automatic Mesh Generation Scheme for Plane and Curved Surfaces by Isoparametric Coordinates", Int.J.Numer.Methods.Eng., Vol. 3, pp. 519-528, 1971

- (23) Kalkani, E.C., "Mesh Generation Program for Highway Excavation Cuts", Int.J.Numer.Methods.Eng., Vol. 8, pp. 369-394, 1974
- (24) Tsai, S.W., "Mechanics of Composite Materials Part II - Theoretical Aspects", Technical Report AFML-TR-66-149 Part II, Air Force Materials Laboratory, Wright Patterson Air Force Base, Ohio, 1966

## Appendix A

### Input Data Files

#### A1. Input Data for NTHICK - Pattern Description

2.04	.0053	24	36						
12	1								
24	2								
1	68	2	133	22	120	36	45	0	0
2.5	180.	48	0						
2.5	187.34	144	40						
14.1	0	42	0						
22.3	0	40	0						
30.4	0	38	0						
38.6	0	35	0						
46.8	0	30	0						
55.0	0	25	0						
63.2	0	20	0						
71.4	0	14	0						
79.5	0	8	0						
86.8	0	2	0						
86.8	0	2	0						
79.5	0	8	0						
71.4	0	14	0						
63.2	0	20	0						
55.0	0	25	0						
46.8	0	30	0						
38.6	0	35	0						
30.4	0	38	0						
22.3	0	40	0						
14.1	0	42	0						
2.5	187.34	144	40						
2.5	180.	48	0						

## A2. Input Data for SPHMESH

```
0
0
.062 .188 .28 2.0 2.647
.04 24 4 4
24
1
1 314
```

## A3. Input Data for COUPLE

Fiber sphere with 24 fiber layers

1,24,1,0

1,0

2,0

3,0

4,0

5,0

6,0

7,0

8,0

9,0

10,0

11,0

12,0

13,0

14,0

15,0

16,0

17,0

18,0

19,0

20,0

21,0

22,0

23,0

24,0

3,2

1,15.6E06,15.6E06,15.6E06,.355,.355,.355,5.8E06

2,12,E06,.5E06,.5E06,.35,.015,.015,185200.

1,5836E04

1,5836E04

1,5836E04

1,5836E04

1,5836E04

1,5836E04

1,5836E04

1,5836E04

1,5836E04

1,5836E04

1,5836E04

1,5836E04

1,5836E04

1,5836E04

1,5836E04

1,5836E04



1,5836E04  
1,5836E04  
1,5836E04  
1,5836E04  
1,5836E04  
1,5836E04  
1,5836E04

## Appendix B

### Partial Output Listing

#### B1. First Polar Position Thickness Profile

Polar Angle (deg)	Composite Thickness (in)
2.6471	0.0996

Layer Thickness (in)	Fiber Orientation Starting (deg)	Angle BETA Finishing (deg)
0.0272	19.1629	0.0000
0.0226	19.1539	0.0000
0.0000	0.0000	0.0000
0.0000	0.0000	0.0000
0.0000	0.0000	0.0000
0.0000	0.0000	0.0000
0.0000	0.0000	0.0000
0.0000	0.0000	0.0000
0.0000	0.0000	0.0000
0.0000	0.0000	0.0000
0.0000	0.0000	0.0000
0.0000	0.0000	0.0000
0.0000	0.0000	0.0000
0.0000	0.0000	0.0000
0.0000	0.0000	0.0000
0.0000	0.0000	0.0000
0.0000	0.0000	0.0000
0.0000	0.0000	0.0000
0.0000	0.0000	0.0000
0.0000	0.0000	0.0000
0.0000	0.0000	0.0000
0.0000	0.0000	0.0000
0.0000	0.0000	0.0000
0.0000	0.0000	0.0000
0.0226	0.0000	19.1539
0.0272	0.0000	19.1629

To convert from in. to mm multiply by 25.4.

## B2. Last Polar Position Thickness Profile

Polar Angle (deg)	Composite Thickness (in)
90.0005	0.2390

Layer Thickness (in)	Fiber Orientation Angle BETA Starting (deg)	Finishing (deg)
0.0106	85.0086	84.9944
0.0029	83.8234	83.8348
0.0106	75.8620	75.8621
0.0106	67.6378	67.6379
0.0106	59.5143	59.5144
0.0106	51.2872	51.2873
0.0106	43.0429	43.0430
0.0106	34.7871	34.7872
0.0106	26.5153	26.5155
0.0106	18.1645	18.1647
0.0106	9.7164	9.7168
0.0105	0.0000	0.0656
0.0105	0.0656	0.0000
0.0106	9.7168	9.7164
0.0106	18.1647	18.1645
0.0106	26.5155	26.5153
0.0106	34.7872	34.7871
0.0106	43.0430	43.0429
0.0106	51.2873	51.2872
0.0106	59.5144	59.5143
0.0106	67.6379	67.6378
0.0106	75.8621	75.8620
0.0029	83.8348	83.8234
0.0106	84.9944	85.0086

To convert from in. to mm multiply by 25.4.

## Appendix C

### NTHICK Input Instructions

A program for the calculation of the fiber helix angles and the thickness profile for the delta-axisymmetric pattern.

Format	Program
(A-Alphanumeric)	Variable
(I-Integer)	Name
(F-Decimal)	

#### A. Control data line

1. Outside radius of spherical form	F	R
2. Thickness factor=thickness of one band	F	TF
3. Number of band sets in the pattern to the limiting meridional position	I	NBS
4. Number of increments of meridional angle to the limiting meridional position	I	MM

#### B. Material stacking sequence control line

1. Band set number	I	IB
2. Material stacking sequence	I	ISS

within a segmented band

=1 Material in band segment  
 closest to axis of symmetry  
 lies nearest the inside radius  
 =2 Material in band segment  
 closest to axis of symmetry  
 lies farthest from the  
 inside radius

Additional B lines as required until IB equals NBS. These lines specify the stacking sequence for all band sets between the previous IB and the current IB. Normally ISS=1 for downwinds and ISS=2 for upwinds. IB on the last line must equal NBS.

#### C. Polar angle increment control line

- |                                   |   |       |
|-----------------------------------|---|-------|
| 1. Integer value of position      | I | IP(I) |
| along the meridian from           |   |       |
| the polar axis                    |   |       |
| 2. The value of M(I) to yield the | I | M(I)  |
| required meridional angular       |   |       |
| increment,                        |   |       |
| =180/M(I) in degrees for the      |   |       |
| region up through IP(I)           |   |       |

Repeat IP(I) and M(I) for a total of five specifications on this line.

Additional C lines as required.

D. Band set data line

One line for each band set in order of winding sequence.

- |   |   |    |
|---|---|----|
| 1. Angle between the polar axis<br>and inner edge of band<br>set in north hemisphere<br>If $OO=0$ : $OI$ =angle between<br>polar axis and center<br>of band<br>If $NB=1$ : $OI$ =one half the<br>band width angle | F | OI |
| 2. Angle between the polar<br>axis and inner edge of band<br>set in south hemisphere  | F | OO |
| 3. Number of bands in this<br>set required for full<br>coverage of the equator  | I | NB |
| 4. Number of bands used in<br>this band set<br>(If equal to NB it may be<br>entered as zero)  | I | NI |

## Appendix D

### SPHMESH Input Instructions

A program for the generation of a finite element mesh across one quarter of a filament wound sphere, such that no element crosses any layer boundaries.

The input to SPHMESH is provided on two Fortran units, one for general control information (unit 15) and one for the thickness profile (unit 12) which is provided by the output from NTHICK.

Format	Program
(A-Alphanumeric)	Variable
(I-Integer)	Name
(F-Decimal)	

The following is for Unit 15 input. There are five data lines (A, B, C, D, E) required.

#### A. Output mode line

- |                               |   |        |
|-------------------------------|---|--------|
| 1. Graphics control option    | I | IGRAPH |
| =0, No graphics               |   |        |
| =1, Plot graphics             |   |        |
| 2. Output control option line | I | IMODE  |
| =0, Normal output with titles |   |        |

=1, Creates output for COUPLE

B. Fill tube geometry line

1. Inside diameter of fill tube	F	D1
2. Outside diameter of fill tube	F	D2
3. Height of fill tube	F	H
4. Inside radius of spherical form	F	YD(1)
5. Starting polar angle of fibers	F	PANG(1)

C. Fill tube and spherical form elements control line

1. Thickness of spherical form	F	TLAY(1,1)
2. Number of elements up fill tube	I	NV
3. Number of elements through fill tube	I	NH
4. Number of elements through spherical form	I	NF

D. Fiber composite elements control line

1. Number of elements in radial direction	I	NR
--	---	----

E. Plot control line

1. Plot control =0, Full plot =1, Partial plot	I	ITETT
2. Starting node number	I	ISTART
3. Finishing node number	I	IFIN



If ITETT=0, entries 2 and 3 may be omitted.

The following is for Unit 12, which is usually provided by the output from NTHICK. There are three control data lines (A, B, C) and NP sets of data lines consisting of a C line and LAYN D lines.

A. Layer control line

1. Number of fiber layers	I	LAYN
---------------------------	---	------

B. Polar position control line

1. Number of polar positions	I	NP
------------------------------	---	----

C. Polar angle and thickness data line

One line for each polar position (NP lines).

1. Polar angle	F	PANG(I)
2. Total fiber thickness	F	TTH

D. Fiber angle and thickness control line

One line for each fiber layer (LAYN lines) at the polar position on the C lines.

1. Layer thickness	F	TLAY(K,I)
2. Starting fiber angle	F	BBETA(I,1)
3. Finishing fiber angle	F	BBETA(I,2)

## Appendix E

### COUPLE Input Instructions

A program for creating the input file for COMPSPH using the output file from SPHMESH. The output file from SPHMESH is read on unit 5 and all other data is read on unit 7. The following describes the input data to be read in on unit 7.

Format	Program
(A-Alphanumeric)	Variable
(I-Integer)	Name
(F-Decimal)	

#### A. Problem title line

1. Problem title to be printed on output	A	HED
---	---	-----

#### B. Control data line

1. Number of element groups	I	NUMEG
2. Number of load cases	I	NLCASE
3. Solution mode =0 data check =1 execution	I	MODEX
4. Nodal load print control =0 does not print	I	NVECT

=1 prints

5. Output suppression control                    I                    NOUT

=0 full output

=1 suppressed output

Note: The suppressed output is the input data, the program generated data, the element stresses for the last load step, the accumulated stresses and the average layer stresses and strains.

#### C. Load case control data line

1. Load case number                                    I                    LL

2. Number of applied concentrated                    I                    NLOAD

nodal loads in this load case

(If NLOAD = 0, omit D lines for  
this load case)

#### D. Load specification lines (NLOAD lines required)

1. Node number where load is                        I                    NOD  
applied

2. Direction of load                                    I                    IDIRN

=1 Load along X axis

=2 Load along Y axis

=3 Load along Z axis

3. Magnitude of load                                    F                    FLOAD

(must include + or -)

## E. Element control data line

1. Element type	I	NPAR(1)
=3 Axisymmetric element		
2. Number of different material property sets	I	NPAR(3)

## F. Material property lines--axisymmetric elements

One line for each material set (maximum of NPAR(3) sets).

1. Property set number	I	N
2. Young's modulus - 1	F	E(1,N)
3. Young's modulus - 2	F	E(2,N)
4. Young's modulus - 3	F	E(3,N)
5. Poisson's ratio - NU-23	F	E(4,N)
6. Poisson's ratio - NU-31	F	E(5,N)
7. Poisson's ratio - NU-21	F	E(6,N)
8. Shear modulus - G-12	F	E(7,N)

where

- 1 Fiber direction
- 2 Lamination plane transverse direction
- 3 Normal to lamination plane direction

NOTE: The above is for orthotropic material. For isotropic material, entries 1, 2 and 5 need to be specified, with zeroes for all other entries.

### G. Initial layer tension lines

One line for each fiber layer.

1. Initial layer tension stress	F	TENS(I)
---------------------------------	---	---------

## Appendix F

### COMSPH Input Instructions

A program for finite element analysis of the fabrication process for filament winding composite spheres. The following is a description of the input data file for COMSPH. This file results from running the other preprocessing programs, i.e., NTHICK, SPHMESH, and then running COUPLE.

Format	Program
(A-Alphanumeric)	Variable
(I-Integer)	Name
(F-Decimal)	

#### A. Problem title line

1. Problem title to be printed on output	A	HED
---	---	-----

#### B. Control data line

1. Number of nodal points	I	NUMNP
2. Number of element groups	I	NUMEG
3. Number of load cases	I	NLCASE
4. Solution mode	I	MODEX

=0 data check

=1 execution

5. Nodal load print control                    I                    NVECT

=0 does not print

=1 prints

6. Output suppression control                  I                    NOUT

=0 full output

=1 suppressed output

Note: The suppressed output is the input data, the program generated data, the element stresses for the last load step, the accumulated stresses and the average layer stresses and strains.

#### C. Nodal point data line

The following set of entries must be entered for each node except for those program generated. Nodal point data lines must be supplied for nodal point numbers 1 and NUMNP. NUMNP must be defined last.

1. Nodal point number (NUMNP max)            I                    N

2. r boundary condition code                  I                    ID(1,N)

=0 Free disp.

=1 Fixed disp.

3. z boundary condition code                  I                    ID(2,N)

=0 Free disp.

=1 Fixed disp.

4. t boundary condition code                  I                    ID(3,N)

=0 Free disp.

=1 Fixed disp.

5. r coordinate	F	X(N)
6. z coordinate	F	Y(N)
7. t coordinate	F	Z(N)
8. Node generation increment	I	KN

#### Automatic nodal point generation

Node point data for a series of nodes (NI, NI+KN, NI+2KN, ... NJ) may be generated from information given on two lines in sequence:

```

LINE I: NI ID(NI,1) ID(NI,2) ID(NI,3) X(NI) Y(NI) Z(NI) KN
LINE J: NJ ID(NJ,1) ID(NJ,2) ID(NJ,3) X(NJ) Y(NJ) Z(NJ)

```

The first generated node will be I+KN, the second will be NI+2KN, etc., until the node number NJ is reached. The difference (NJ-NI) must be evenly divisible by KN. The boundary condition codes on the generated nodes will be the same as those on line I. The coordinates will be linearly interpolated.

Multiple load cases may be run by inputting a set of D and E data lines for each load case. The number of load cases entered must agree with the value of NLCASE previously specified on B control data line. Each load case will produce a separate solution for truss and plate bending problems. Results from each load case are added to those



accumulated in the previous load steps to produce one total accumulative solution for axisymmetric problems.

#### D. Load case control data line

- |  |   |       |
|--|---|-------|
| 1. Load case number  | I | LL    |
| 2. Number of applied concentrated<br>nodal loads in this load case<br>(If NLOAD = 0, omit E lines for<br>this load case) | I | NLOAD |

#### E. Load specification lines (NLOAD lines required)

- |  |   |       |
|--|---|-------|
| 1. Node number where load is<br>applied  | I | NOD   |
| 2. Direction of load<br>=1 Load along r axis<br>=2 Load along z axis<br>=3 Load along t axis | I | IDIRN |
| 3. Magnitude of load<br>(must include + or -)  | F | FLOAD |

#### F. Element control data line

- |   |   |         |
|---|---|---------|
| 1. Element type<br>=3 Axisymmetric element        | I | NPAR(1) |
| 2. Number of elements                             | I | NPAR(2) |
| 3. Number of material or section<br>property sets | I | NPAR(3) |

### G. Material property lines--axisymmetric elements

One line for each material set (maximum of NPAR(3) sets).

1. Property set number	I	N
2. Young's modulus - 1	F	E(1,N)
3. Young's modulus - 2	F	E(2,N)
4. Young's modulus - 3	F	E(3,N)
5. Poisson's ratio - NU-23	F	E(4,N)
6. Poisson's ratio - NU-31	F	E(5,N)
7. Poisson's ratio - NU-21	F	E(6,N)
8. Shear modulus - G-12	F	E(7,N)

where

- 1 Fiber direction
- 2 Lamination plane transverse direction
- 3 Normal to lamination plane direction

NOTE: The above is for orthotropic material. For isotropic material, entries 1, 2 and 5 need to be specified, with zeroes for all other entries.

### H. Element data lines--axisymmetric elements

One line for each element not program generated.

Element input must begin with element number 1 and end with the last element number. Elements will be generated between every pair of nonconsecutive element number data lines.

1. Element number	I	M
-------------------	---	---

2. Node number	I	I
3. Node number	I	J
4. Node number	I	K
5. Node number	I	L
6. Material set number	I	MTYP
7. Node generation increment	I	KG
8. IOFFON number	I	IOFFON(M)
9. Initial element hoop stress	F	TENS(M)
10. Fiber angle	F	BETA(M)
11. Polar position angle	F	SETA(M)

Nodes must be numbered counterclockwise around the element.

To form triangular elements, make node number L equal to node number K.

#### Automatic element generation

If 2 consecutive element data lines skip any element numbers, then elements M to M+N will be generated. Node numbers will be incremented by KG. Element numbers and IOFFON(M) will be incremented by 1 for all generated elements.

LINE 1: M I J K L MTYP KG IOFFON(M) TENS(M)

LINE 2: M+N I+NP J+NP K+NP L+NP MTYP IOFFON(M+N) TENS(M+N)

Where NP = N\*KG

The MTYP and initial stress on the generated elements will be the same as on line 1.

## I. Average layer strain control data line

1. Number of layers	I	LAYN
---------------------	---	------

One set of the following for each layer. LAYN sets of one J line followed by K data lines for all elements in the layer.

## J. Last element number control data line

1. Last element number in layer	I	ISEN
---------------------------------	---	------

## K. Fiber length data line

One line for each element in layer.

1. Fiber length in each element	F	ELEM(M)
---------------------------------	---	---------

Appendix G  
COMSPH Program Outline

MAIN

- 1) Zero's master array.
- 2) Read in master heading (HED), total number of nodal points (NUMNP), total number of element groups (NUMEG), number of load cases (NCASE), solution mode (MODEX = 1 execution ; = 0 data check only) and loading vector option (NVECT = 1 print nodal load vector; = 0 does not print nodal load vector).
- 3) Assign permanent storage locations in the master A array for the boundary condition ID array, N1 = 1 through N2 = N1 + 3 \* NUMNP.
- 4) Assigns temporary storage locations in A for the nodal coordinates. N2 through N3 = N2 + NUMNP \* ITWO for X, N3 through N4 = N3 + NUMNP \* ITWO for Y and N4 through N5 = N4 + NUMNP \* ITWO for Z. (ITWO = 2 for double precision)

Calls subroutine INPUT

- 1) Reads in nodal point coordinates and boundary condition codes (ID array).
- 2) A final ID array is constructed from the given ID

array, such that fixed degrees of freedom are eliminated and each free nodal degree of freedom corresponds to an equation in the final system of equations.

- 3) Writes out complete nodal point data; node number, condition code (ID array) and coordinates.
- 4) Calculates NEQ, the total number of equations.
- 5) Saves the nodal point coordinates temporarily in the assigned storage locations N2 through N5 of array A.

Return to MAIN

- 5) Assigns temporary storage locations in A for the load vector R, N5 through N6 = N5 + NEQ \* ITWO.
- 6) Reads in the load case number (LL) and the number of concentrated loads applied in this case (NLOAD).
- 7) Assigns temporary storage locations in A for the concentrated loads, N6 through N7 = N6 + NLOAD, for the nodes at which loads are prescribed. N7 through N8 = N7 + NLOAD for the directions of the prescribed loads and N8 through N9 = N8 + NLOAD \* ITWO for the magnitudes of the prescribed loads.

Calls subroutine LOADS

- 1) Reads in load information.
- 2) Writes out load information.
- 3) Calculates the assembled load vector R.
- 4) Dumps the R vector onto tape ILOAD.

Return to MAIN

- 7) Clears storage locations N5 through N6 = N5 + NEQ.
- 8) Sets flag IND = 1, to read and store element information for each element group.

Calls subroutine ELCAL

- 1) Read in element type (NPAR(1) = 3 axisymmetric elements). The number of elements in this group (NPAR(2) = NUME) and the number of different sets of material properties (NPAR(3) = NUMMAT).

Calls subroutine ELEMNT

- 1) Calls appropriate subroutine for the specified element type. The following assumes Type = 3 axisymmetric

elements.

Calls subroutine TRING

- 1) Assigns temporary storage locations in A, starting at N101 = N6. Locations N101 through N102 = N101 + NUMMAT \* ITWO \* 7 for material properties; locations N102 through N103 = N102 + NUME \* ITWO \* 4 for initial tensile stresses; locations N103 through N104 = N103 + NUME \* 12 for the LM connectivity arrays for each element; locations N104 through N105 = N104 + NUME \* ITWO \* 12 for the nodal point coordinates; locations N105 through N106 = N105 + NUME for the material types, MATP; locations N106 through N107 = N106 + NUME for the IOFFON option, IOFFON; locations N107 through N108 = N107 + NUME \* ITWO \* 4 for the cumulative stresses in r-z-t coordinates, STRESS; locations N108 through N109 = N108 + NUME \* 4 for the node numbers to which the internal nodal forces are applied, NNE; locations N109 through N110 = N109 + NUME \* ITWO \* 8 for the internal nodal forces, TDD; locations N110 through N111 = N110 + NEQ \* ITWO for the internal load vector, RI; locations N111 through N112 = N111 + NUME \* ITWO for the fiber angle, BETA; locations N112 through N113 = N112 + NUME \* ITWO for the polar angle,



SETA; locations N113 through N114 = N113 + NUME \* ITWO \* 4 for the stresses per load step in r-z-t coordinates, STTR; locations N114 through N115 = N114 + NUME \* ITWO \* 6 for the fiber coordinates, 1-2-3, strains per load step, SSTTR; locations N115 through N116 = N115 + NUME \* 4 for the cumulative 1-2-3 stresses, FSTRES; locations N116 through N117 = N116 + NUME \* ITWO \* 6 for strains in r-z-t coordinates per load step, STRN; locations N117 through N118 = N117 + NUME \* ITWO \* 6 for the 1-2-3 stresses per load step, STRES; locations N118 through N119 = N118 + NUME \* ITWO \* 6 for the cumulative 1-2-3 strain, TSTRAN; locations N119 through N120 = N119 + NUME \* ITWO for the initial tensile stress, TTENS; locations N120 through N121 = N120 + NUME \* ITWO for the average stress in the fiber direction, 1, ASTRAN; locations N121 through N122 = N121 + NUME \* ITWO \* 6 for the average strain in the fiber direction, 1, ASTRES; and finally locations N122 through N123 = N122 + NUME \* ITWO for the fiber lengths in the elements, ELEM.

Calls subroutine RING

- 1) Reads in material property set number, N; material properties, E.

- 2) Reads in element number, M; element connectivity, II, JJ, KK, LL; material type, MTYP; element generation node number increment, KG; IOFFON option number, IOFFON; initial stresses, TENS; fiber angle, BETA; and the polar angle, SETA.
- 3) Assigns nodes to which the internal nodal forces are applied.
- 4) Calculates the LM array.

Calls subroutine COLHT

- 1) Calculates and updates the MHT array, stored in locations N5 through N6 = N5 + NEQ. The MHT array provides the column heights in the structure stiffness matrix.

Return to RING

- 5) Writes out element information.

Return to TRING

Return to ELEMNT

Return to ELCAL

- 2) Dumps all information in storage locations N101 through N107 onto tape IELMNT.
- 3) Dumps all information in storage locations N107 through N108 onto tape ISTRES.
- 4) Dumps all information in storage locations N108 through N109 onto tape IILoad.
- 5) Dumps all information in storage locations N109 through N123 onto tape IANGLE.

Return to MAIN

Calls subroutine ADDRES

- 1) This subroutine uses the MHT array now in storage locations N5 through N6 to construct the array MAXA which stores the locations of the diagonal elements of the assembled stiffness matrix in a skyline fashion to facilitate the storage of the structure stiffness matrix in the one dimensional A array.
- 2) Calculates the mean band width MK.
- 3) Calculates the total storage locations, NWK, required

for the assembled stiffness matrix.

Return to MAIN

- 10) Stores the MAXA array permanently in the A array in locations N2 through N3 = N2 + NEQ + 1.
- 11) Assigns storage locations N3 through N4 = N3 + NWK \* ITWO for the assembled stiffness matrix; locations N4 through N5 = N4 + NEQ \* ITWO for the load vector, R; and locations N5 through N6 = N5 + (N101 + N107).
- 12) Begins Do loop to analyze all load cases. In the fabrication sequence modeling each additional layer that causes the next group of elements to be turned on becomes the next load case.
- 13) Zeroes the A array from A(N3) through A(NNL).
- 14) Set flag IND = 2, to compute element stiffness matrices for each element group.

Calls subroutine ASSEM

- 1) Reads tape IELEMNT.
- 2) Reads tape ISTRES.
- 3) Reads tape IILoad.
- 4) Reads tape IANGLE.

Calls subroutine ELEMNT

Calls subroutine TRING

- 1) Assigns temporary storage locations N101 through N118 as before.

Calls subroutine RING

Calls subroutine FTRAN

- 1) Transforms the initial stress array from the 1-2-3 system to the s-t-n system by rotation about the third axis through the angle BETA.
- 2) Permutates the s-t-n system to n-s-t.
- 3) Transforms the initial stress array from the n-s-t system to the r-z-t system by rotation about the third axis through the angle (90-SETA).

Return to RING

Calls subroutine SUM

- 1) Calculates the Jacobian matrix.
- 2) Calculates the B matrix and it's transpose.

Calls subroutine MATSTF

- 1) If the element in this load case has not been turned on by its IOFFON value then the material properties are reduced by the order of 10E6 to render the element stiffness insignificant, but without numerical difficulties.
- 2) If the element fiber direction stress during the previous load step became negative (indicating total tension loss), the fiber direction modulus is reduced to the value of the transverse modulus thus greatly reducing the element stiffness when tension is lost in the uncured composite.
- 3) Calculates the D matrix for the element in fiber, 1-2-3, coordinates.

Calls subroutine TRAN

- 1) Transforms the D matrix from the 1-2-3 system to the

s-t-n system by rotation about the third axis through the angle BETA..

- 2) Permutates the s-t-n system to the n-s-t.
- 3) Transforms the D matrix from the n-s-t system to the r-z-t system by rotation about the third axis through the angle (90-SETA).

Return to MATSTF

Return to SUM

- 3) Calculates the matrix product BDB.

Return to RING

- 3) Calculates the element stiffness matrix using a two point Gauss Quadrature routine.

Calls subroutine SUM

- 1) Calculates the Jacobian matrix.
- 2) Calculates the B matrix and it's transpose.

Calls subroutine MATSTF

- 4) Calculates the D matrix as before, then reduces the fiber, 1, and transverse, 2, stiffnesses by 10E6 in the layer of elements turned on in this load case for the calculation of nodal loads from the initial stress array.

Calls subroutine TRAN

- 1) Transforms the D matrix from the 1-2-3 system to the r-z-t system.

Return to MATSTF

Return to SUM

- 3) Calculates the reduced matrix product BDB.

Return to RING



- 6) Calculates the nodal loads from the initial stress array.
- 7) Forms the upper triangular portion of the element stiffness matrix in the column array S.

Calls subroutine ADDBAN

- 1) Assembles the element stiffness matrix with the structure stiffness matrix.

Return to RING

- 8) Forms the nodal load vector, RI, of internally calculated nodal loads.

Return to TRING

Return to ELEMNT

Return to ASSEM

Return to MAIN

- 15) Sets flag  $KTR = 1$ , for decomposition of the structure stiffness matrix.

Calls subroutine COLSOL

- 1) With  $KTR = 1$ , COLSOL decomposes the assembled stiffness matrix (stored in A locations N3 through N4) and destroys the original assembled matrix.
- 2) Stores the diagonal matrix and the upper triangular matrix in the storage locations N3 through N4.

Return to MAIN

- 16) Sets flag  $KTR = 2$ , for solving the system equation for each load case.
- 17) Sets flag  $IND = 3$ , for calculating element stresses.

Calls subroutine LOADV

- 1) Reads tape ILOAD.
- 2) Adds the external nodal loads to the internal nodal loads for the nodal loads to be applied in this load

step.

Return to MAIN

Calls subroutine COLSOL

- 3) With  $KTR = 2$ , COLSOL uses the diagonal and upper triangular matrices to back substitute and solve the system of equations. The results are stored in locations N4 through N5.

Return to MAIN

Calls subroutine WRITE

- 1) Writes out the displacements.

Return to MAIN

Calls subroutine STRESS

- 1) Reads tapes IELEMNT and ISTRESS.

2) Reads tapes ILOAD and IANGLE.

Calls subroutine ELEMNT

Calls subroutine TRING

Calls subroutine RING

Calls subroutine FTRAN

1) Transforms the initial stress array from the 1-2-3 system to the r-z-t system.

Return to RING

Calls subroutine MATSTF

- 1) If element is not turned on properties are reduced by 10E6.
- 2) If fiber, 1, stress is negative fiber, 2, modulus is reduced.
- 3) Calculates the D matrix as before.

Calls subroutine TRAN

- 1) Transforms the D matrix from the 1-2-3 system to the r-z-t system.

Return to MATSTF

Return to RING

- 9) With IND = 3, recalculates the element stiffness matrix.
- 10) Using the nodal displacements with the element stiffness matrix, calculates the element stresses in the r-z-t system.
- 11) Calculates the element strains in the r-z-t system.

Calls subroutine STRAN

- 1) Transforms the element strains from the r-z-t system to the n-s-t system by rotation about the third axis through the angle SETA.
- 2) Permutates the n-s-t system to the s-t-n system.

- 3) Transforms the element strains from the s-t-n system to the 1-2-3 system by rotation about the third axis through the angle  $(90 - \text{BETA})$ .

Return to RING

- 12) Calculates the element stresses in the fiber coordinate system 1-2-3.
- 13) Writes out stresses in both the r-z-t and 1-2-3 coordinate systems.

On the last load step the following is carried out.

- 14) The layer number, last element number in the layer and the fiber lengths for all elements in the layer.
- 15) Averages strain in each layer using the fiber lengths.
- 16) Writes out the average fiber direction stress and strain for each layer.

Return to TRING

Return to ELEMNT

Return to STRESS

- 2) Backspace tapes IELMNT and ISTRES.
- 3) Rewrite element data with updated geometry onto tape IELMNT.
- 4) Write accumulated stresses onto tape ISTRESS.
- 5) Backspace tapes IILOAD and IANGLE.
- 6) Rewrite load and transformation angles onto tapes IILOAD and IANGLE.

Return to MAIN

18) Proceeds to next load case.

End of program.

**The vita has been removed from  
the scanned document**



AN ANALYTICAL MODEL OF STRENGTH LOSS IN  
FILAMENT WOUND SPHERICAL VESSELS

by

Peter Joseph Leavesley

(ABSTRACT)

The ability to predict potential strength degradation of a filament wound sphere was developed using an incremental finite element model of the composite during fabrication. The sphere was modeled taking into account the winding/loading pattern and the resulting internal layer boundaries. The thickness profile of the sphere's layers were computed using a thickness profile/pattern simulation program. This thickness profile was used by the mesh generating program to ensure that the elements generated did not cross layer boundaries. The elements used were four noded isoparametric quadrilateral elements and these were collapsed to triangular elements for transitions. The input to the finite element program was prepared by an interface program which combines the mesh generator output with the loading and option control data. The main feature of the finite element program was the incremental construction and loading of the model. Strength degradation definitely occurs when the average fiber layer strain is negative. The negative strain means that all the winding tension has been

lost from the layer and the fibers in uncured resin will buckle when they try to support compressive loading. Then when the resin cures the buckled region of fibers are degraded in strength. This model gives a layer-by-layer analysis of the potential strength loss of the composite.